

การตรวจสอบการดูดซับและสภาพเลือกจำเพาะของคาร์บอนไดออกไซด์บนซีโอไลติกอิมิดาโซเลต  
เฟรมเวิร์ก-78 โดยการจำลองพลวัตเชิงโมเลกุล

นางสาวสุนทรีย์ พวงจำปี

วิทยานิพนธ์นี้เป็นส่วนหนึ่งของการศึกษาตามหลักสูตรปริญญาวิทยาศาสตรมหาบัณฑิต

สาขาวิชาปิโตรเคมีและวิทยาศาสตร์พอลิเมอร์

คณะวิทยาศาสตร์ จุฬาลงกรณ์มหาวิทยาลัย

ปีการศึกษา 2554

ลิขสิทธิ์ของจุฬาลงกรณ์มหาวิทยาลัย

บทคัดย่อและแฟ้มข้อมูลฉบับเต็มของวิทยานิพนธ์ตั้งแต่ปีการศึกษา 2554 ที่ให้บริการในคลังปัญญาจุฬาฯ (CUIR)

เป็นแฟ้มข้อมูลของนิสิตเจ้าของวิทยานิพนธ์ที่ส่งผ่านทางบัณฑิตวิทยาลัย

The abstract and full text of theses from the academic year 2011 in Chulalongkorn University Intellectual Repository(CUIR)  
are the thesis authors' files submitted through the Graduate School.

INVESTIGATING ADSORPTION AND SELECTIVITY OF CO<sub>2</sub> ON ZEOLITIC  
IMIDAZOLATE FRAMEWORK-78 USING MOLECULAR DYNAMIC SIMULATION

Ms. Suntharee Phuangjumpee

A Thesis Submitted in Partial Fulfillment of the Requirements  
for the Degree of Master of Science Program in Petrochemistry and Polymer Science

Faculty of Science

Chulalongkorn University

Academic Year 2011

Copyright of Chulalongkorn University



สุนทรีย์ พวงจำปี : การตรวจสอบการดูดซับและสภาพเลือกจำเพาะของคาร์บอนไดออกไซด์บนซีโอไลติกอิมิดาโซเลตเฟรมเวิร์ก-78 โดยการจำลองพลวัตเชิงโมเลกุล.

(INVESTIGATING ADSORPTION AND SELECTIVITY OF CO<sub>2</sub> ON ZEOLITIC IMIDAZOLATE FRAMEWORK-78 USING MOLECULAR DYNAMIC SIMULATION) อ. ที่ปรึกษาวิทยานิพนธ์หลัก : ศ.ดร. สุพจน์ หารหนองบัว, อ. ที่ปรึกษาวิทยานิพนธ์ร่วม : ดร. อรพรรณ แสงสว่าง, 55 หน้า.

การแยก แก๊ส คาร์บอนไดออกไซด์ออกจาก แก๊ส ธรรมชาติซึ่งมี แก๊ส มีเทนเป็นองค์ประกอบหลักเป็นกระบวนการที่สำคัญในอุตสาหกรรมปิโตรเคมี โดย ZIF-78 ถือเป็นวัสดุหนึ่งที่ได้รับ ความสนใจในการนำมาใช้เพื่อการแยกคาร์บอนไดออกไซด์ออกจาก แก๊สผสม โดยงานวิจัยนี้จะศึกษาพฤติกรรมของการดูดซับจำเพาะและการแพร่จำเพาะใน ระดับโมเลกุลของแก๊สผสมระหว่างคาร์บอนไดออกไซด์ และมีเทนด้วย ZIF-78 โดยใช้ระเบียบวิธีแกรนด์ คานอนิคอล มอนติคาร์โล และการจำลองพลวัตเชิงโมเลกุล ผลจาก RDF พบว่า แก๊สคาร์บอนไดออกไซด์ถูกดูดซับที่อะตอม ออกซิเจนของหมู่ไนโตร (-NO<sub>2</sub>) ของ ZIF-78 และแก๊สมีเทนถูกพบมากที่สุดที่บริเวณอะตอมไฮโดรเจนของตัวเชื่อมต่อกับไนโตรอิมิดาโซเลต (nlm) ส่วนค่าการแพร่ของแก๊สคาร์บอนไดออกไซด์นั้นไม่ขึ้นกับความเข้มข้น ในขณะที่ค่าการแพร่ของแก๊สมีเทนขึ้นอยู่กับความเข้มข้น และพบว่าค่าการดูดซับจำเพาะ (8.08) มีค่ามากกว่าค่าการแพร่จำเพาะ (~0.3) อย่างเห็นได้ชัด ซึ่งแสดงให้เห็นว่าการดูดซับจำเพาะมีบทบาทสำคัญมากกว่าการเลือกผ่านของเมมเบรน ดังนั้นการใช้ ZIF-78 สำหรับการแยกในรูปแบบสมดุลดีกว่าการแยกแบบเมมเบรน

สาขาวิชา ปิโตรเคมีและวิทยาศาสตร์พอลิเมอร์ ปลายมือชื่อ  
 ปีการศึกษา.....2554..... ปลายมือชื่อ อ.ที่ปรึกษาวิทยานิพนธ์หลัก.....  
 ปลายมือชื่อ อ.ที่ปรึกษาวิทยานิพนธ์ร่วม .....

# # 5272591023 : PETROCHEMISTRY AND POLYMER SCIENCE

KEYWORDS : ZIF-78 / SIMULATION / ADSORPTION / DIFFUSION / SELECTIVITY

SUNTHAREE PHUANGJUMPEE : INVESTIGATING ADSORPTION AND  
SELECTIVITY OF CO<sub>2</sub> ON ZEOLITIC IMIDAZOLATE FRAMEWORK-78 USING  
MOLECULAR DYNAMIC SIMULATION. ADVISOR : PROF. SUPOT  
HANNONGBUA, Dr.rer.nat., CO-ADVISOR : ORAPHAN SAENGSAWANG,  
Dr.rer.nat., 55 pp.

The removal of CO<sub>2</sub> from natural gas that mainly contributed by CH<sub>4</sub> is most important elementary step in up-stream petroleum industry. ZIF-78 is a promising material for the separation of CO<sub>2</sub> from a gas mixture. In this work, the molecular behavior of CO<sub>2</sub> and CH<sub>4</sub> in ZIF-78 as well as the adsorption selectivity and diffusion selectivity of CO<sub>2</sub> in CO<sub>2</sub>/CH<sub>4</sub> mixtures were investigated using Grand Canonical Monte Carlo (GCMC) and molecular dynamic (MD) simulations. The RDF results show that the CO<sub>2</sub> is strongly adsorbed at O atoms of the –NO<sub>2</sub> group of ZIF-78 whereas the CH<sub>4</sub> is mostly observed at H atoms of the nitroimidazolate linker of ZIF-78, respectively. The self diffusivity of CO<sub>2</sub> does not depend on the concentration but it is the case for CH<sub>4</sub>. From both kinds of selectivity, the significantly higher of adsorption selectivity (8.08) than diffusion selectivity (~0.3) indicates the main contribution of adsorption selectivity in membrane permeability. It demonstrates that using ZIF-78 in equilibrium-based separation will be more efficient than using them in membrane-based separation applications.

Field of Study : Petrochemistry and Polymer Science Student's Signature.....

Academic Year : .....2011..... Advisor's Signature.....

Co-advisor's Signature.....

## ACKNOWLEDGEMENTS

This work would not be possible without person who support and encourage. I would like to express my appreciation to all these who gave me the possibility to complete this thesis.

Firstly, I would like to thanks my family for all their support. Especially, my father who supports me throughout. Furthermore, I would like to gratefully thanks my advisor Prof. Dr. Supot Hannongbua and co-advisor Dr. Oraphan Saengsawang for all advices and helps. I also would like to thanks Prof. Dr. Siegfried Fritzsche, Dr. Rungroj Chanajaree and Assoc. Prof. Dr. Vudhichai Parasuk for several nice suggestions, discussion.

I would like to thanks Prof. Dr. Pattarapan Prasassrakich, Asst. Prof. Dr. Somsak Pianwanit and Dr. Arthorn Loisuangsinn who act as the thesis committee.

Finally, I would like to acknowledge the Thailand Research Fund (TRF:RTA 4980006), the Deutsche Forschungsgemeinschaft (Schwerpunktprogramm SPP 1392), the National Research University Project of CHE and the Ratchadaphiseksomphot Endowment Fund (AM1078I) for the financial support and also the Asian Development Bank (ADB) scholarship, Petrochemical and Polymer science, Chulalongkorn University for all support. The Computational Chemistry Unit Cell (CCUC) at Department of Chemistry, Faculty of science, Chulalongkorn University is acknowledged for all computer resource and other facilities.

## CONTENTS

	<b>Page</b>
<b>ABSTRACT IN THAI.....</b>	<b>iv</b>
<b>ABSTRACT IN ENGLISH.....</b>	<b>v</b>
<b>ACKNOWLEDGEMENTS.....</b>	<b>vi</b>
<b>CONTENTS.....</b>	<b>vii</b>
<b>LIST OF TABLES.....</b>	<b>x</b>
<b>LIST OF FIGURES.....</b>	<b>xi</b>
<b>LIST OF ABBREVIATIONS.....</b>	<b>xiii</b>
<b>CHAPTER I INTRODUCTION.....</b>	<b>1</b>
1.1 Motivation.....	1
1.2 Separation of CO <sub>2</sub> from CO <sub>2</sub> and CH <sub>4</sub> mixtures.....	2
1.3 Zeolitic imidazolate frameworks (ZIFs).....	2
1.3.1 Application.....	3
1.3.2 Zeolitic imidazolate frameworks-78 (ZIF-78).....	4
1.3.3 Properties of Zeolitic imidazolate frameworks-78 (ZIF-78).....	5
1.4 Literature review.....	5
1.5 Scope of this study.....	7
<b>CHAPTER II THEORETICAL BACKGROUND.....</b>	<b>8</b>
2.1 Grand canonical Monte Carlo simulations.....	8

	<b>Page</b>
2.2 Molecular dynamics simulations.....	11
2.3 Comparing GCMC and MD simulations.....	14
2.4 Molecular simulation techniques.....	14
2.4.1 Periodic boundary conditions.....	14
2.4.2 Lennard-Jones and Coulomb pair potential.....	15
2.4.3 Long-ranged interactions.....	17
2.4.4 Radial distribution functions.....	17
2.4.5 Self-diffusion coefficient.....	18
<b>CHAPTER III CALCULATION DETAILS.....</b>	<b>19</b>
3.1 ZIF-78 structure preparation.....	19
3.2 Force field parameterization.....	20
3.3 Molecular dynamic simulation.....	23
3.4 Evaluation.....	24
3.4.1 Radial distribution functions.....	24
3.4.2 Probability density in z direction.....	25
3.4.3 Self-diffusion coefficient.....	26
3.4.4 Adsorption selectivity.....	27
3.4.5 Diffusion selectivity.....	27
3.4.6 Membrane selectivity.....	27
3.4.7 Knudsen selectivity.....	28
<b>CHAPTER IV RESULTS AND DISCUSSION.....</b>	<b>29</b>
4.1 Validation of guest-host interaction parameter.....	29



	<b>Page</b>
4.2 Structure of CO <sub>2</sub> and CH <sub>4</sub> in ZIF-78 lattice.....	30
4.2.1 Radial distribution functions, RDFs.....	30
4.2.2 Probability density.....	33
4.3 Self diffusion.....	35
4.4 Adsorption selectivity.....	37
4.5 Diffusion selectivity.....	38
4.6 Membrane permeability.....	39
<b>CHAPTER V CONCLUSIONS.....</b>	<b>40</b>
<b>REFERENCES.....</b>	<b>41</b>
<b>APPENDICES.....</b>	<b>45</b>
APPENDIX A: Module used in Material Studio Program for this thesis.....	46
<b>CURRICULUM VITAE.....</b>	<b>55</b>

## LIST OF TABLES

<b>Table</b>		<b>Page</b>
1.1	Compositions of natural gas found in Thailand.....	2
1.2	Properties of ZIF-78.....	5
2.1	The difference between GCMD and MD simulation.....	14
3.1	Lennard-Jones potential parameters for adsorbate-adsorbate and adsorbate-ZIF interactions.....	21
3.2	The intermolecular interactions obtained from the Lorentz-Berthelot mixing rules	22
4.1	The calculated diffusion selectivity of CO <sub>2</sub> in CO <sub>2</sub> /CH <sub>4</sub> mixture at different ratios	38

## LIST OF FIGURES

Figure	Page
1.1 The bridge of metal by imidasolate where IM denotes imidasolate ring.....	3
1.2 Crystal structures of ZIF-78.....	4
2.1 Step of calculation of adsorption isotherm in GCMC simulations.....	10
2.2 All type of potential ( $U$ ).....	12
2.3 Step of calculation in MD simulations.....	13
2.4 The periodic boundary condition.....	15
2.5 Lennard-Jones function.....	16
2.6 The volume of annular $\Delta V(r)$ .....	17
3.1 Crystal structures of the ZIF-78 used in the simulations (a) $1 \times 1 \times 1$ unit cells and (b) $2 \times 2 \times 2$ unit cells.....	19
3.2 Atomic partial charges of (a) ZIF-78 (b) $\text{CO}_2$ and (c) $\text{CH}_4$ .....	20
3.3 Adsorption isotherm from the experiment.....	23
3.4 Part of ZIF-78 structure and the atomic label.....	24
3.5 The ZIF-78 in each axis.....	25
3.6 An example of mean square displacement.....	26
4.1 The calculated adsorption isotherm at 298 K for $\text{CO}_2$ and $\text{CH}_4$ in comparison to that obtained experimentally.....	29
4.2 Two types of linker, <i>i.e.</i> , nitroimidazolate (Type I) and nitrobenzimidazolate (Type II) coordinated to Zn ion are shown. The atomic labels are also given.....	30
4.3 RDFs from ZIF-78 to atoms of $\text{CO}_2$ , $i_{\text{ZIF}} - j_{\text{CO}_2}$ where $i$ are the atoms of ZIF-78 (see Figure 4.2 for label) and $j$ represents the atoms of $\text{CO}_2$ .....	31
4.4 RDFs from ZIF-78 to atoms of $\text{CH}_4$ , $i_{\text{ZIF}} - j_{\text{CH}_4}$ , where $i$ are the atoms of ZIF-78 (see Figure 4.2 for label) and $j$ represents the atoms of $\text{CH}_4$ .....	32
4.5 Schematic of the adsorption sites of (a) $\text{CO}_2$ (yellow) and (b) $\text{CH}_4$ (green) in ZIF-78.....	33

<b>Figure</b>	<b>Page</b>
4.6 The snapshot of (a) 10 molecules of CO <sub>2</sub> and (b) 5 molecules of CH <sub>4</sub> in ZIF-78, as well as probabilities density in z-direction of (c) 10 molecules of C atom of CO <sub>2</sub> , (d) 5 molecules of C atom of CH <sub>4</sub> , (e) 10 molecules of O atom of CO <sub>2</sub> , (f) 5 molecules of H atom of CH <sub>4</sub> . Here, the dash line show the edges of lattice channel.....	34
4.7 The probability density in z-direction for (a) C atom of CO <sub>2</sub> and (b) C atom of CH <sub>4</sub> for various concentrations.....	35
4.8 The calculated MSD with loading dependence of (a) CO <sub>2</sub> and (b) CH <sub>4</sub> in ZIF-78.....	35
4.9 The self diffusivity with loading dependence of (a) CO <sub>2</sub> and (b) CH <sub>4</sub> in ZIF-78.....	36
4.10 (a) Adsorption isotherm of CO <sub>2</sub> and CH <sub>4</sub> calculated from GCMC simulation of equimolar mixture at 298 K, as well as, (b) the corresponding adsorption selectivity calculated from Eq. (3.7) at different pressure.....	37
4.11 Adsorption selectivity, diffusion selectivity, and membrane permeability of ZIF-78 for CO <sub>2</sub> /CH <sub>4</sub> .....	39

## LIST OF ABBREVIATIONS

ZIFs	=	Zeolitic imidazolate frameworks
ZIF-78	=	Zeolitic imidazolate framework-78
MOF	=	Metal organic framework
Im	=	Imidazolate
nIm	=	2- nitroimidazolate
nbIm	=	5- nitrobenzimidazolate
LJ	=	Lennard-Jones
GCMC	=	Grand canonical monte carlo
MD	=	Molecular dynamic
PW91	=	Perdew Wang 91
DND	=	Double numerical basis set plus d function
GGA	=	Generalized gradient approximations
DFT	=	Density functional theory
ESP	=	Electro static potential fitting
Å	=	Angstrom
K	=	Kelvin
kPa	=	kiloPascal
ns	=	nanosecond
fs	=	femtosecond
RDF	=	Radial distribution function
MSD	=	Mean square displacement

# CHAPTER I

## INTRODUCTION

### 1.6 Motivation

Adsorption is one of the methods that are commonly used to separate mixtures or contaminations in raw materials. Even a small amount of the contamination was found to disturb the processes, damage the devices or, reduce the quality of products, *e.g.*, in the natural gas industry, which contains a high percentage of CH<sub>4</sub>, the CO<sub>2</sub> must be separated, otherwise it can cause pipe corrosion.

To date, there are many materials used to separate CO<sub>2</sub> from gas mixtures, *e.g.*, poly membrane, zeolites, metal organic frameworks (MOFs) and zeolitic imidazolate frameworks (ZIFs). ZIFs have high thermal, chemical stability and also a large variety of ZIF structures. Thus, ZIFs are a new promising candidate for this application [1-3]. Banerjee *et al.* [4] studied physical properties that control of pore size and functionality in isoreticular zeolitic imidazolate frameworks and their carbon dioxide selective capture properties. The results showed that ZIF-78 is the most effective CO<sub>2</sub> adsorbent and shows the highest selectivity for CO<sub>2</sub> from binary mixtures that include CH<sub>4</sub>, N<sub>2</sub>, and O<sub>2</sub>. Phan *et al.* [5] collect the data of synthesis, structure, and carbon dioxide capture properties of zeolitic imidazolate frameworks. They also found that ZIF-78 is the material that shows highest CO<sub>2</sub> capture and has the highest selectivity for the CO<sub>2</sub> separation from binary mixtures.

Although, experimental data have already shown that ZIF-78 is one of the best material for adsorption and separation applications. However, understanding of adsorption and diffusion of CH<sub>4</sub> and CO<sub>2</sub> in micro- or nano-porous materials at molecule level is also very important. This, then, becomes the rational good of their study. Here, adsorption and diffusion of CO<sub>2</sub> and CH<sub>4</sub> in ZIF-78 were investigated using GCMC and MD simulations.

## 1.7 Separation of CO<sub>2</sub> from CO<sub>2</sub> and CH<sub>4</sub> mixtures

**Table 1.1** Compositions of natural gas found in Thailand [6].

Gas type	Texas Pacific	Bongkoch
Methane	58.39	65.71
Ethane	4.98	5.03
Propane	2.45	2.48
Butanes	1.02	1.2
C <sub>5</sub> and higher	0.37	0.7
N <sub>2</sub>	0.78	0.91
CO <sub>2</sub>	32	23.97

As seen in Table 1.1, natural gas contains a high percentage of CH<sub>4</sub> as well as CO<sub>2</sub>. Moreover, in case of cryogenic processes at reduced temperature and increased pressure, CO<sub>2</sub> becomes solid which, then, reduces the heating efficiency and also takes up volume in the pipeline. These effects lead to very high maintenance cost per year. In addition separation of CO<sub>2</sub> from landfills gas which arises from fermentation helps also to reduce the greenhouse effect. This CH<sub>4</sub> recovering process also helps to reduce the use of fossil fuels [7].

## 1.8 Zeolitic imidazolate frameworks (ZIFs)

ZIFs are porous material, a novel subfamily of metal organic frameworks (MOFs). They are composed of a tetrahedral cluster of MN<sub>4</sub> units (M = Zn, Cu, Co, etc.) covalently joined by bridging simple imidazolate (Im) and its derivative ligands ( see Figure 1.1).

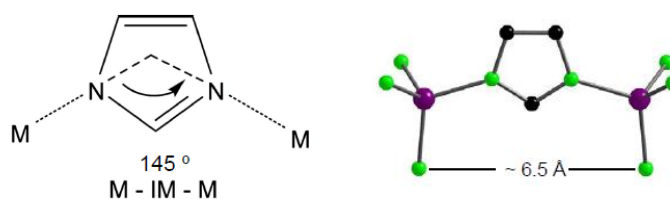


**Figure 1.1** The bridge of metal by imidazolate [8] where IM denotes imidazolate ring.

The properties of ZIFs with a remarkably low density, potentially large surface area and many sites available for gas adsorption as well as chemical and thermal stability are considered as great candidates for gas storage and gas separation applications.

### 1.3.1 Applications

#### 1.3.1.1 Catalysis

The porous material becomes a promising targets as catalyst in petrochemical industry because it has a high surface area, *e.g.*, zeolite used as catalyst in olefin polymerization industrial. For ZIFs, ZIF-8 is the most promising one. It was synthesized and used as an efficient heterogeneous catalyst for the Knoevenagel reaction [9].

#### 1.3.1.2 Gas Storage

This is a consequence of its large surface area, chemical and thermal stability and many sites available for gas adsorption. For example, ZIF-8 and ZIF-11 [3, 10-13] were used to storage  $H_2$ . In addition, ZIFs was very interesting for storage of  $CO_2$ . Yaghi and his team synthesized 25 ZIFs crystal structures, three of which showed a particular affinity for capturing carbon dioxide (ZIF-68, ZIF-69, ZIF-70). They found that one litre of the crystals could store  $\sim 83$  litres of  $CO_2$  [14].



### 1.3.1.3 Gas separation

ZIF membranes can be used for the separation of gases, *e.g.*, ZIF-8 membrane is one which has high CO<sub>2</sub> permeability for equimolar mixtures of CO<sub>2</sub>/CH<sub>4</sub> and also shows high H<sub>2</sub>/CH<sub>4</sub> selectivity [15-17]. On the other hand, the selectivity studies of ZIF-68, -69, -70, -78, -79, -80, -81 and -82 found that ZIF-78 has the highest selectivity for CO<sub>2</sub> from binary mixtures [4].

### 1.3.2 Zeolitic imidazolate frameworks-78 (ZIF-78)

ZIF-78 has a GME (gmelinite) topology with Zn linked by mixed imidazolate linker, which is 2- nitroimidazolate (nIm) and 5- nitrobenzimidazolate (nbIm) (Figure 1.2).

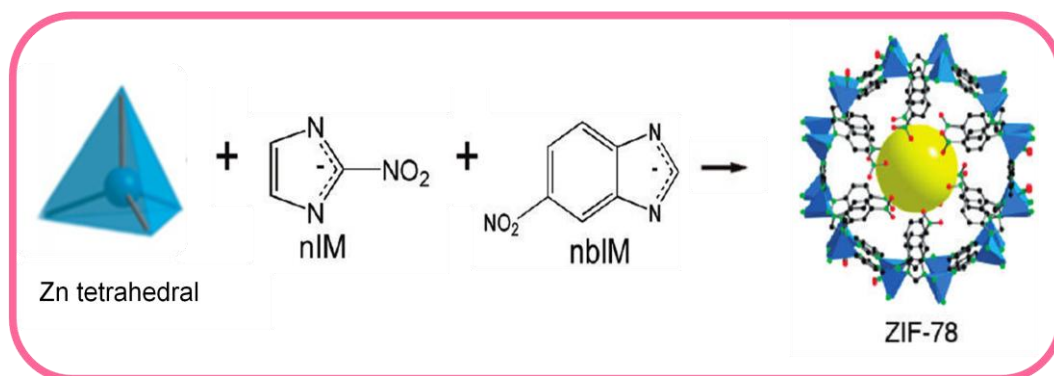


**Figure 1.2** Crystal structures of ZIF-78 [4].

### 1.3.3 Properties of zeolitic imidazolate frameworks-78 (ZIF-78)

**Table 1.2** Properties of ZIF-78.

Material	ZIF-78
Unit cell ( $\text{\AA}$ ) <sup>a</sup>	a = 26.1174, b = 26.1174, c = 19.4910
Cell angle (deg) <sup>a</sup>	$\alpha = 90$ $\beta = 90$ $\gamma = 129$
Zeolite topology <sup>b</sup>	gmelinite (GME)
Volume ( $\text{\AA}^3$ ) <sup>b</sup>	11,514
Density ( $\text{g/cm}^3$ ) <sup>a</sup>	1.198
Surface area ( $\text{m}^2/\text{g}$ ) <sup>b</sup>	620
Pore Diameters( $\text{\AA}$ ) <sup>b</sup>	7.1
Pore Apertures( $\text{\AA}$ ) <sup>b</sup>	3.8

<sup>a</sup> from XRD crystal data [4], <sup>b</sup> from ref [5].

The polar functional group in ZIF-78 makes it possible for polar gas adsorption. Another advantage of ZIF-78 are thermal stability ( $\sim 390$  °C) and chemical stability (boiling benzene, methanol and water for 7 days). [4]

## 1.9 Literature review

In 2009, Banerjee *et.al* [4] studied the factors that control the pore size and functionality in isorecticular zeolitic imidazolate frameworks and their carbon dioxide selective capture properties. The results show that ZIF-78 is the most effective CO<sub>2</sub> adsorbent and has the highest

selectivity for CO<sub>2</sub> from binary mixtures that include CH<sub>4</sub>, N<sub>2</sub>, and O<sub>2</sub>. Their experiments have also indicated that CO<sub>2</sub> uptake capacity was influenced primarily by functionality effects rather than pore metrics.

In 2009, Liu *et al* [18] studied adsorption and diffusion behavior of CO<sub>2</sub> in ZIF-68 and ZIF-69 using GCMC and MD simulations. The calculation results indicated that the small pores formed by the nIm linkers in ZIF-68 and ZIF-69 were the preferential sites for CO<sub>2</sub> adsorption at low pressure. This work demonstrates that the chlorine atoms in 5-chlorobenzimidazolate (cbIm) linkers in ZIF-69 lead to enhanced adsorption of CO<sub>2</sub>.

In 2009, Andrew *et al* [19] studied the nature of guest binding sites and selectivity in the ZIF-68 and ZIF-69 by GCMC and MD simulations. The results found that the CO<sub>2</sub> molecules associate strongly with the benzene rings of benzimidazolate anion and the binding energies of CO guests in the lattice are much smaller than those of CO<sub>2</sub>. They also found that the size of the guest and aperture size in lattice affect the diffusion rates considerably.

In 2009, Rankin *et al* [20] studied the adsorption and diffusion of light gases in ZIF-68 and ZIF-70 using geometries obtained from density functional theory (DFT) optimization. The framework charges obtained from Bader charge decomposition (periodic DFT calculations) and ChelpG charges (cluster DFT calculations). The results found that the N<sub>2</sub> adsorption isotherms in ZIF-68 and ZIF-70 are well agreement with experiment when charge-quadrupole interaction (CQI) terms are included. In contrast, the simulations over predict the amount of CO<sub>2</sub> adsorbed at 298 K compared with experiments.

In 2010, Phan *et al* [5] collect the data of synthesis, structure, and carbon dioxide capture properties of zeolitic imidazolate frameworks. They found that ZIF-78 is material that shows the highest for CO<sub>2</sub> capture and has the highest selectivity for CO<sub>2</sub> from binary mixtures.

In 2010, Hou *et al* [21] calculated uptake and selectivity of CO<sub>2</sub> in ZIF-68 and ZIF-69. Calculation results indicate that the strong Lewis acid–base interaction exists between the gas molecules and nitro groups of nIm linkers and the stacking of gas molecules in the small pores thus preventing the further entry of gas molecules. The large pores of ZIFs are the key to controlling adsorption ability of ZIFs because O atoms of CO<sub>2</sub> can interact with the H atoms of

the phenyl rings in large pores. The presence of electron withdrawing groups in the phenylimidazole linker of ZIF increases the interaction between the O atoms of CO<sub>2</sub> and H atoms of the phenyl rings in its large pore.

In 2010, Smit *et al* [22] studied the separation of CO<sub>2</sub>/N<sub>2</sub>, CO<sub>2</sub>/CH<sub>4</sub>, and CH<sub>4</sub>/N<sub>2</sub> by ZIF-68 and ZIF-69 using GCMC simulation. The results show that ZIF-69 is more beneficial for separating CO<sub>2</sub> than ZIF-68, due to the presence of chlorine atoms in cbIm linkers. The overall separation performances of these two ZIFs for separating the chosen mixtures are comparable to typical MOFs and zeolites.

In 2011, Keskin [23] studied atomic simulation for adsorption, diffusion and separation of CH<sub>4</sub>/H<sub>2</sub>, CO<sub>2</sub>/CH<sub>4</sub> and CO<sub>2</sub>/H<sub>2</sub> in ZIF-3 and ZIF-10. The results suggest that using ZIF-3 and ZIF-10 in equilibrium-based separation processes will be more efficient than using them in membrane-based separation applications because the adsorption selectivity is higher than the permeation selectivity for all cases. And the results also found that the separation performances of ZIFs are comparable to other MOFs.

## 1.10 Scope of this study

1.5.1 GCMC simulations were used to calculate the adsorption isotherm, which is used to validate the parameterization, and also used to calculate the adsorption selectivity.

1.5.2 MD simulations were used to study the radial distribution function (RDF), the probability to find number of guest molecule in z direction, the self-diffusion coefficient and the diffusion selectivity, where:

1.5.2.1 The ratio that is used to calculate the membrane permeability, which is calculated from the diffusion selectivity and the adsorption selectivity, is 1:1 at 298 K 101.3 kPa.

1.5.4 Loadings of the guest molecule in MD simulations at 298 K are 10, 80, 150, 220 molecules for CO<sub>2</sub> and 5, 25, 45, 65 molecules for CH<sub>4</sub>.

## CHAPTER II

### THEORETICAL BACKGROUND

Computer simulations aim to understand the structural and dynamical properties of assemblies of molecules based on their microscopic interactions. Simulations are mainly used in comparison with experiments, and can also be used to test the theoretical developments based on the same model. The simulation can be performed at extreme temperatures or pressures, which are difficult or impossible to achieve in a laboratory. The details of molecular motions, which are invisible for the experiment, can be obtained from the simulations [24]. In this work, the Grand canonical Monte Carlo simulations were carried out to obtain the adsorption isotherms of the guest molecules in ZIF-78, in order to validate the force field parameter and obtain the adsorption selectivity. Then, the validated force field parameters were used for the molecular dynamics simulations to obtain the dynamical properties of guest molecules in ZIF-78 e.g. the self-diffusion coefficient, the diffusion selectivity, etc.

#### 2.1 Grand canonical Monte Carlo simulations

The adsorption isotherm explains the number of guest molecules inside the porous materials as a function of pressure at the given temperature. It can be obtained from the Monte Carlo (MC) simulations [25] with the Grand canonical ensemble [26]. In this ensemble, the chemical potential  $\mu$ , the volume  $V$ , and the temperature  $T$  are constant, whereas, the number of particles  $N$  can fluctuate during the simulations. This is achieved by means of trial insertion and deletion of molecules. The procedure is set up with equal probability for the process of guest molecule displacement, insertion, and deletion. A trial particle is first randomly chosen whether an insertion or deletion is attempted. If insertion is chosen, a particle is placed with uniform probability density inside the system. If deletion is chosen, one particle out of  $N$  particles is randomly deleted. Then, the trial move is then accepted or rejected according to the usual MC procedure. The acceptance criterion of a displacement from an initial configuration ( $v_1$ ) to a generated configuration by MC move ( $v_2$ ) is

$$w_{\tau \rightarrow \tau'} = \min\left\{1, \exp\left(-\frac{\Delta E}{kT}\right)\right\} \quad (2.1)$$

where  $\Delta E$  is the differential of total potential energy of the system.

The acceptance probability for insertion is

$$w_{N \rightarrow N+1} = \min\left\{1, \frac{PV}{(N+1)kT} \exp\left(-\frac{\Delta E}{kT}\right)\right\} \quad (2.2)$$

And the probability for gas removal from the solid ZIF phase is given by

$$w_{N \rightarrow N-1} = \min\left\{1, \frac{PV}{(N+1)kT} \exp\left(-\frac{\Delta E}{kT}\right)\right\} \quad (2.3)$$

The steps of GCMC are following as Figure 2.1

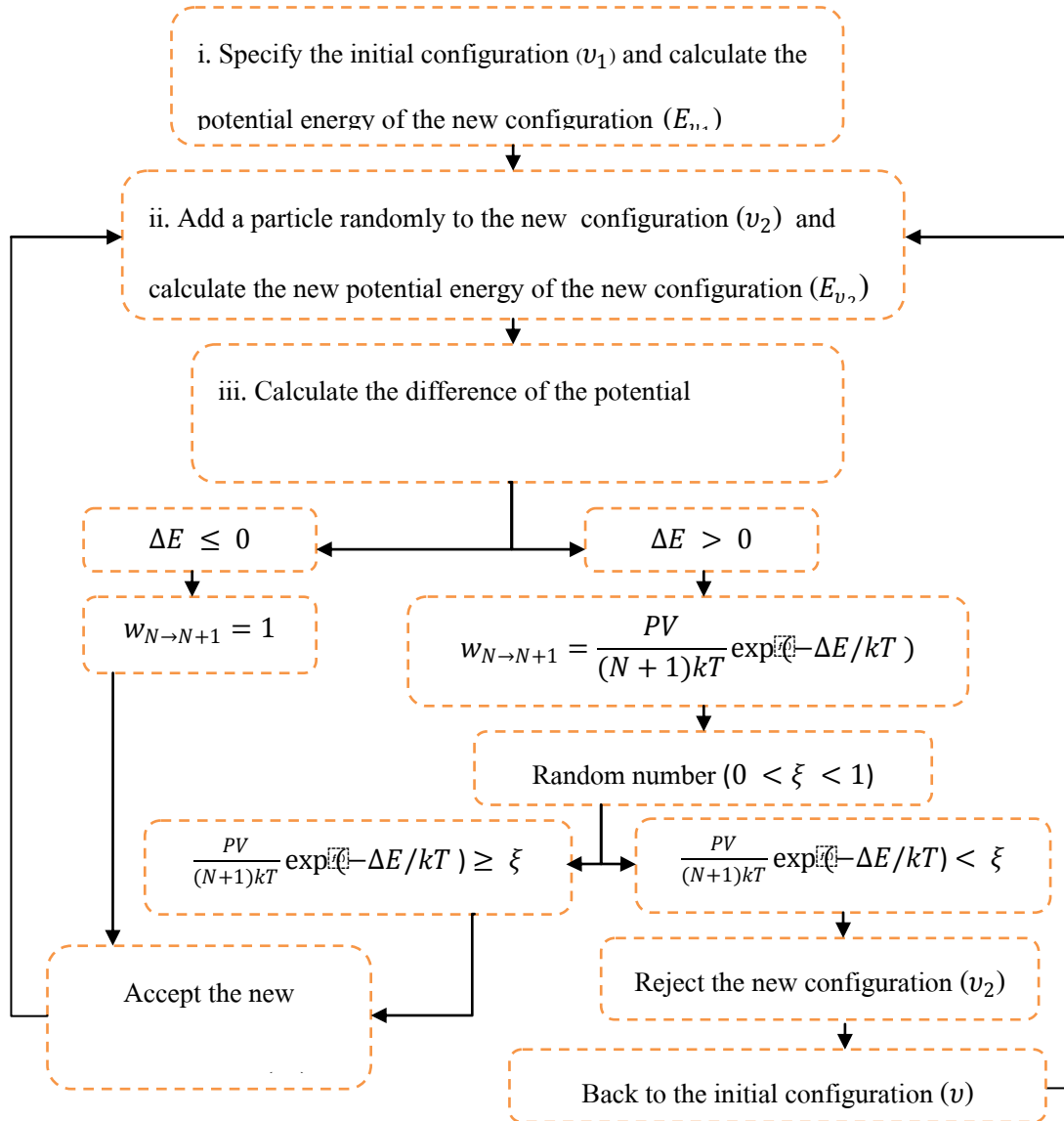


**Figure 2.1** Step of calculation of adsorption isotherm in GCMC simulations [26].

- i. Specify the initial configuration ( $v_1$ ) in term of Cartesian coordinate system and calculate the potential energy of the initial configuration ( $v_1$ ), which assume to be  $E_{v_1}$
- ii. Add a particle randomly to the new Cartesian coordinate system as same as new configuration ( $v_2$ ) and calculate the potential energy of the new initial configuration ( $v_2$ ), which assume to be  $E_{v_2}$

iii. Calculate the difference of the potential energy of the configuration

( $\Delta E = E_{v_2} - E_v$ ) and consider the acceptance of the new configuration by

→ If  $\Delta E \leq 0$  mean the new configuration is stability than the old one. Thus, accept the new configuration.

→ If  $\Delta E > 0$  give the chance to accept new configuration by

consider  $w_{N \rightarrow N+1}$ , where

$$w_{N \rightarrow N+1} = \frac{PV}{(N+1)kT} \exp\left(-\frac{\Delta E}{kT}\right).$$

To consider the  $w_{N \rightarrow N+1}$ , the random number ( $\xi$ ), where

( $0 < \xi < 1$ ) were random and comparing with

$w_{N \rightarrow N+1}$

→ If  $w_{N \rightarrow N+1} \geq \xi$  accept the new configuration.

→ If  $w_{N \rightarrow N+1} < \xi$  reject the new configuration.

iv. Repeat the iii step unit the potential energy of system decrease to stability.

v. Collect the data.

vi. Analyze the data, which is adsorption isotherm [25-26].

## 2.2 Molecular dynamics simulations

The molecular dynamics simulation (MD) technique was developed by Alder and Wainwright [27] in 1957 in order to simulate the behavior of an ensemble of hard spheres depending on the thermodynamics conditions. This was a field of current investigation at that time among statistical mechanism specialists. MD is used to study the structural and dynamical properties on a molecular scale, through the solution of the classical equation of motion for classical particles representing the atoms and molecules of a chemical system.

The particles usually interact through a potential, which in most investigations, is taken to be the sum of suitable pair potentials, depending on the distances between particles. The forces acting on the particles are evaluated from the derivative of the potentials, and Newton's law of motion is applied (see Eq. (2.4) and Eq. (2.5))

$$F_i(t) = m_i a_i(t) = m_i \frac{\partial v_i}{\partial t} = \frac{\partial x_i^2}{\partial t} \quad (2.4)$$



where  $F_i$  can be obtained through Eq. (2.5)

$$F_i = -\frac{\partial U(r)}{\partial r_i} \quad (2.5)$$

Where  $F_i(t)$  is force acting on atom  $i$  at time  $t$ .

$m_i$  is mass of atom  $i$ .

$a_i$  is acceleration of atom  $i$  at time  $t$ .

$v_i$  is velocity.

$x_i$  is coordinate.

$U$  is potential energy.

The potential energy is expressed as

$$U = U_{bond} + U_{nonbond} \quad (2.6)$$

Where  $U_{bonded} = U_{bond} + U_{angel} + U_{dihedral}$

$U_{non-bonded} = U_{VDW} + U_{Coulomb}$

All type of potential ( $U$ ) was shown in Figure 2.2.

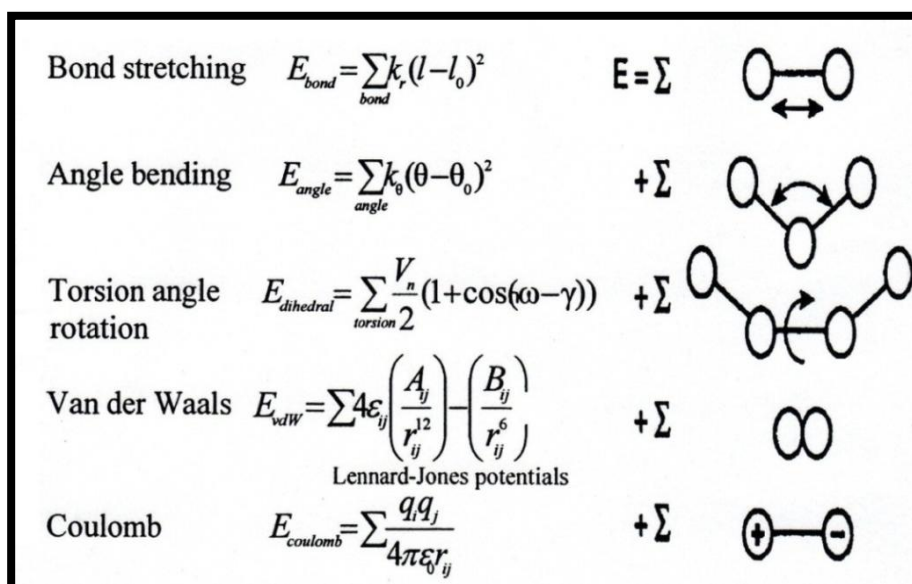
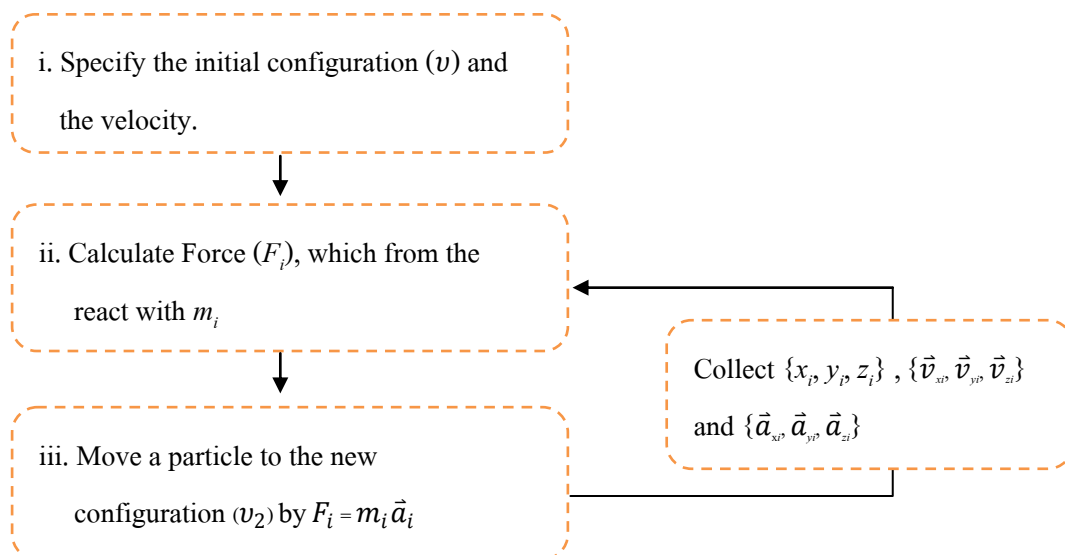


Figure 2.2 All type of potential ( $U$ ) [28].

There are many different force fields exist. *e.g.*, UFF [29] and DREIDING [30] and in case of  $U_{VDW}$  Forcefield was using from paper of Liu *et al.* [18]

The steps of MD are following as Figure 2.3.



**Figure 2.3** Step of calculation in MD simulations [31].

- i. Specify the initial configuration ( $\mathbf{U}$ ) and velocity in term of Cartesian coordinate system.
- ii. Calculate Force ( $F_i$ ), which from the react with  $m_i$
- iii. Move a particle to the new Cartesian coordinate system as same as new configuration ( $u_2$ ) by  $F_i = m_i \vec{a}_i$
- iv. Repeat the ii step unit the potential energy of system decrease to stability.
- v. Collect the data.
- vi. Analyze the data. This might be radial distribution function, concentration profile and Self-diffusion coefficient [29].

The statistical averages of interest are calculated from the positions and the velocities of the particles as time averages over the trajectories of the system in its phase space. Since it is possible to calculate the forces acting on all particles from the potential, which is assumed to be

known. Unfortunately, an analytical solution for the resulting system of equations is not possible in general since the motion of one particle is affected by all other particles. However, the time integration algorithms e.g. velocity Verlet algorithm [32], the leap-frog algorithm [33], and the Beeman algorithm [34], etc, have been developed to predict positions, velocities, and accelerations.

### 2.3 Comparing GCMC and MD simulations

To compare GCMC and MD simulations, Table 2.1, which express the difference between GCMC and MD simulations, are shown.

**Table 2.1** The difference between GCMC and MD simulation [25,31].

GCMC	MD
1. Only one atom was moved randomly.	1. All atoms were moved by equation of motion ( $F = ma = m \frac{\partial v}{\partial t} = m \frac{\partial^2 x}{\partial t^2}$ ).
2. The lattice and guest molecules are treated as rigid.	2. The lattice and guest molecule can be treated as rigid or flexible.
3. Stochastic movement and independence on time.	3. Deterministic movement and depend on time.
4. Potential energy is the determination for stability system .	4. Potential energy, pressure, temperature and force can be the determination for stability system.

### 2.4 Molecular simulation techniques

#### 2.4.1 Periodic boundary condition

To model a macroscopic system by a finite simulation system of  $N$  particles, the concept of periodic boundary conditions is introduced. The simulation box is replicated in all directions to

give a periodic array. In Figure 2.4, the two dimensional box is surrounded by eight neighbor box. When the atom moves through a boundary, it is replaced by its corresponding images entering from the opposite side; therefore, the number of particles in the system is constant.

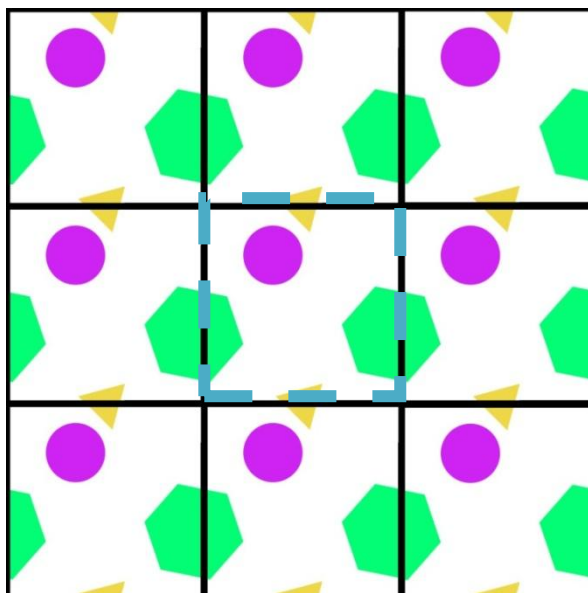


**Figure 2.4** The periodic boundary condition.

In the simulations, there are non-bonded interactions i.e. intermolecular interactions or intramolecular interactions between particles. To deal with these non-bonded interactions efficiently, the cutoff radius is applied with the concept of the minimum image convention. In the minimum image convention, the energy and force are calculated only for the shortest distance between a particle  $i$  and a particle  $j$  or one of its images  $j'$ . When the spherical cutoff is applied, the interactions between particles, which are not in the cutoff radius, are set to zero. When the minimum image convention is also used, this cutoff radius must be equal or less than half of the smallest box edge [35].

#### 2.4.2 Lennard-Jones and Coulomb pair potential

The intermolecular interactions are described by pairwise-additive Lennard-Jones potentials [36] as shown in Eq. (2.7).

$$u(r_{ij}) = 4\varepsilon_{ij} \left[ \left( \frac{\sigma_{ij}}{r_{ij}} \right)^{12} - \left( \frac{\sigma_{ij}}{r_{ij}} \right)^6 \right] \quad (2.7)$$

The  $\left( \frac{\sigma_{ij}}{r_{ij}} \right)^{12}$  term of the equilibrium is responsible for small distance repulsion and the  $-\left( \frac{\sigma_{ij}}{r_{ij}} \right)^6$  term provides an attractive term which approaches zero as the distance between the two atoms increased [36].

The  $\sigma$  and  $\varepsilon$  parameters for each atom pair are obtained using Lorentz-Berthelot mixing rules[37] as shown in Eq. (2.8) and Eq. (2.9).

$$\sigma_{ij} = (\sigma_{ii} + \sigma_{jj})/2 \quad (2.8)$$

$$\varepsilon_{ij} = \sqrt{\varepsilon_{ii}\varepsilon_{jj}} \quad (2.9)$$

Figure 2.5 shows a representation of Lennard-Jones 12-6 function

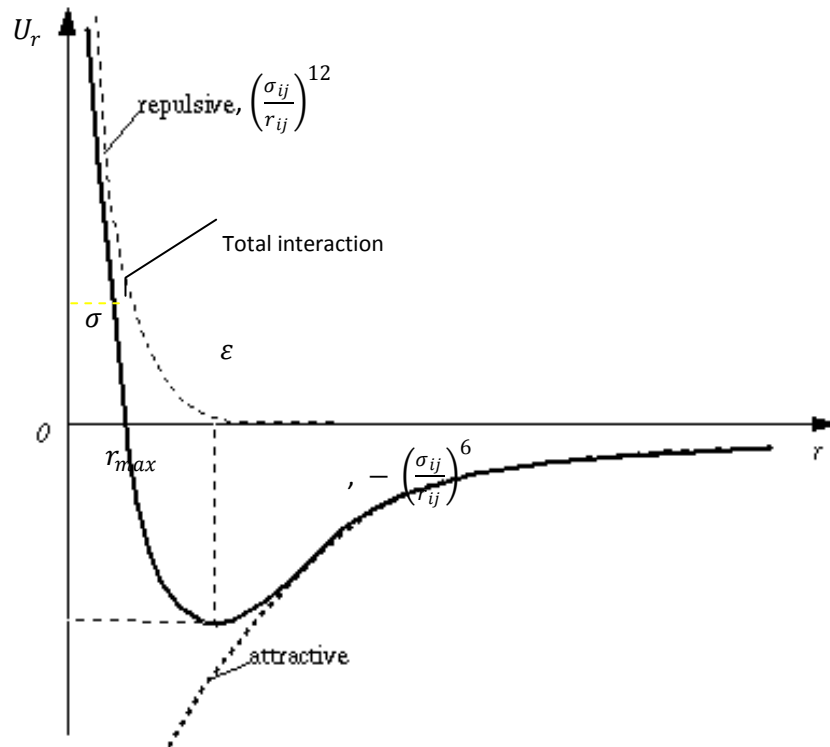


**Figure 2.5** Lennard-Jones function.

### 2.4.3 Long-ranged interactions

The charge-charge interactions, which decay as  $1/r$ , are long ranged. It is problematic in molecular simulations. Therefore, the long-ranged electrostatic interactions were handled using the Ewald summation technique [38]. The Ewald summation is the most rigorous technique for calculating electrostatic interaction in a periodic system, but it is computationally quite expensive.

### 2.4.4 Radial distribution functions

To describe the structural averages, the radial distribution function (RDF) is used. The RDF is one of the tools in statistical mechanics that demonstrate a probability to find a particle at distance  $r$  away from a given reference particle. It is expressed by the average number of particles in each shell at distance  $r$  from any determined atom and normalized by dividing by the number of particles, by the volume of each shell and the average density of particles in the system; see Figure 2.6 and Eq. (2.10) [25,31].

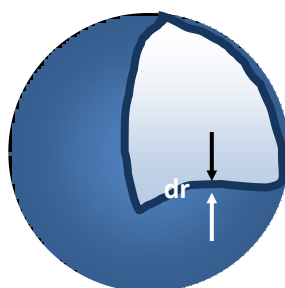


**Figure 2.6** The volume of annular  $\Delta V(r)$ .

$$g_{ij}(r) = \frac{N(r)}{\rho_{ij} \Delta V(r)} \quad (2.10)$$

Where  $\Delta V(r)$  is the volume of annular.  
 $N(r)$  is the number of atom, which found in volume of annular  $\Delta V(r)$ .  
 $\rho_{ij}$  is the number density of all pair  $ij$  that found in simulation cube,  
 which the volume is  $V$ .

### 2.4.5 The Self-diffusion coefficient

The self-diffusion coefficient ( $D_s$ ) is the displacement of the tagged particle (or molecules) in the absence of concentration gradient. It can be obtained from the NMR measurements [26] or from the slope of the mean square displacement (MSD). The relation between  $D_s$  and the MSD is given by the Einstein's relation:

$$D_s = \frac{1}{6N} \sum_{i=1}^N \langle [r_i(t) - r_i(0)]^2 \rangle \quad (2.11)$$

where  $N$  is the number of diffusive atoms in the system.

$\sum_{i=1}^N \langle [r_i(t) - r_i(0)]^2 \rangle$  is Mean square displacement (MSD), which is the account of the positions of an atom for a period of time[39].

## CHAPTER III

### CALCULATION DETAILS

Both GCMC and MD were calculated using the Material Studio package [40]. The GCMC simulations used the *Sorption* module whereas, the MD simulations used the *Forcite* module in Material Studio packages.

#### 3.1 ZIF-78 structure preparation

One unit cell of the ZIF-78 structure was obtained from the X-ray crystallographic data [4] and it was, then, extended to the simulation boxes used in GCMC and MD simulations having the size of  $1\times 1\times 1$  and  $2\times 2\times 2$  unit cells, respectively. The MD simulations have been carried out at 298 K for the loadings of guest molecules of 10, 65, 80, 150, 220 molecules for  $\text{CO}_2$  and 5, 25, 45, 65 molecules for  $\text{CH}_4$ .

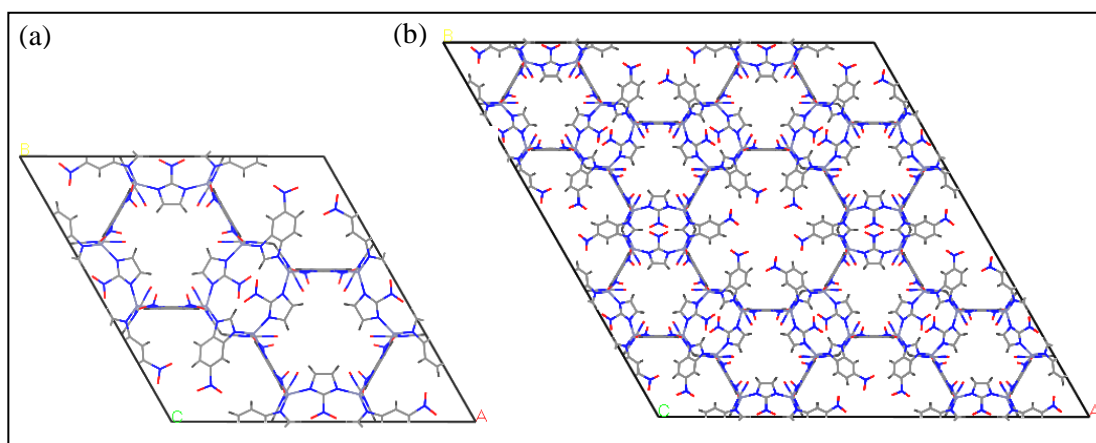


**Figure 3.1** Crystal structures of the ZIF-78 used in the simulations (a)  $1\times 1\times 1$  unit cells and (b)  $2\times 2\times 2$  unit cells.



### 3.2 Force field parameterization

To validate the force field applied, the GCMC simulations were used to calculate the adsorption isotherm of CO<sub>2</sub> and CH<sub>4</sub> molecules in ZIF-78 under the pressure of 0 – 110 kPa and at 298 K. The adsorption isotherms were also used to calculate the adsorption selectivity. Here, the ZIF-78 lattice was treated as rigid during the simulation and only one unit cell is sufficient to represent the physical properties in the adsorption isotherm.

The Lennard-Jones potential parameters with the columbic potentials parameter were used to calculate the intermolecular interactions between CH<sub>4</sub>, CO<sub>2</sub> and ZIF-78. All the partial charges were extracted by DFT calculation using *Accelrys Dmol<sup>3</sup>*, Material Studio packages. The partial charges of ZIF-78, CO<sub>2</sub> and CH<sub>4</sub> were calculated using the PW91 GGA density functional and the double numerical basis set plus d-functions (DND) and electro-static potential fitting (ESP).

The Lennard-Jones parameters and the partial charges of ZIF-78, CO<sub>2</sub> and CH<sub>4</sub> are shown in Figure 3.2 and Table 3.1.

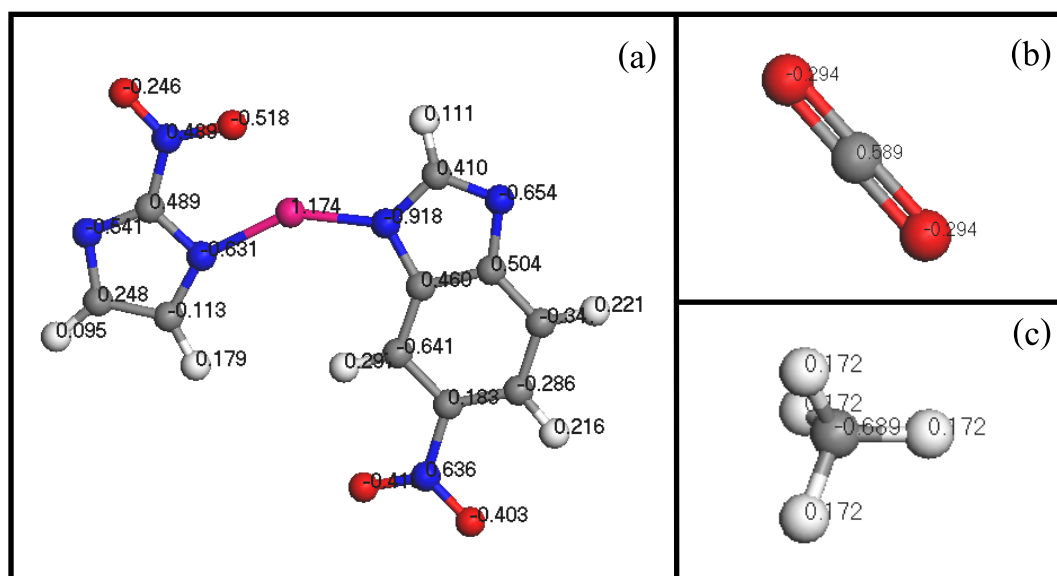


**Figure 3.2** Atomic partial charges of (a) ZIF-78 (b) CO<sub>2</sub> and (c) CH<sub>4</sub>

**Table 3.1** Lennard-Jones potential parameters for adsorbate-adsorbate and adsorbate-ZIF interactions.

<b>Atom</b>	<b>Atom-atom <math>\sigma</math> (Å)<sup>a</sup></b>	<b>Atom-atom <math>\epsilon/k_B</math> (K)<sup>a</sup></b>	<b>Atom-atom <math>\epsilon</math> (kcal/mol)</b>
<b>ZIF_C</b>	3.43	52.84	0.1050
<b>ZIF_O</b>	3.12	30.19	0.0600
<b>ZIF_N</b>	3.26	34.72	0.0690
<b>ZIF_H</b>	2.57	22.14	0.0440
<b>ZIF_Zn</b>	2.46	62.4	0.1240
<b>CO<sub>2</sub>_C</b>	3.43	52.84	0.1050
<b>CO<sub>2</sub>_O</b>	3.12	30.19	0.0600

<sup>a</sup> Taken from Liu *et al.*[9].

The intermolecular interactions are described by the pairwise-additive Lennard-Jones potentials as Eq. (2.7) as mentioned in chapter 2.

The  $\sigma$  and  $\epsilon$  parameters for each atomic pair are obtained using the Lorentz-Berthelot mixing rules as Eq. (2.8) and Eq. (2.9) as mentioned in chapter 2.

**Table 3.2** The intermolecular interactions obtained from the Lorentz-Berthelot mixing rules.

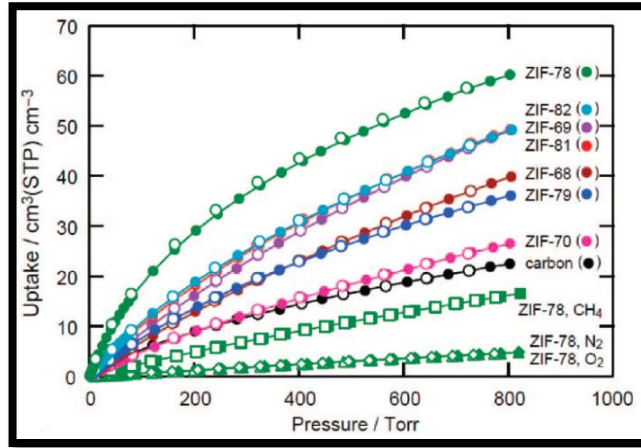
A )		ZIF_C	ZIF_O	ZIF_N	ZIF_H	ZIF_Zn	CO <sub>2</sub> _C	CO <sub>2</sub> _O
	$\epsilon$	0.1050	0.0600	0.0690	0.0440	0.1240	0.1050	0.0600
ZIF_C	0.1050	0.1050	-	-	-	-	-	-
ZIF_O	0.0600	0.0794	0.0600	-	-	-	-	-
ZIF_N	0.0690	0.0851	0.0643	0.0690	-	-	-	-
ZIF_H	0.0440	0.0680	0.0514	0.0551	0.0440	-	-	-
ZIF_Zn	0.1240	0.1141	0.0863	0.0925	0.0739	0.1240	-	-
CO <sub>2</sub> _C	0.1050	0.1050	0.0794	0.0851	0.0680	0.1141	0.1050	-
CO <sub>2</sub> _O	0.0600	0.0794	0.0600	0.0643	0.0514	0.0863	0.0794	0.0600

B )		ZIF_C	ZIF_O	ZIF_N	ZIF_H	ZIF_Zn	CO <sub>2</sub> _C	CO <sub>2</sub> _O
	$\sigma$	3.430	3.120	3.260	2.570	2.460	3.430	3.120
ZIF_C	3.430	3.430	-	-	-	-	-	-
ZIF_O	3.120	3.275	3.120	-	-	-	-	-
ZIF_N	3.260	3.345	3.190	3.260	-	-	-	-
ZIF_H	2.570	3.000	2.845	2.915	2.570	-	-	-
ZIF_Zn	2.460	2.945	2.790	2.860	2.515	2.460	-	-
CO <sub>2</sub> _C	3.430	3.430	3.275	3.345	3.000	2.945	3.430	-
CO <sub>2</sub> _O	3.120	3.275	3.120	3.190	2.845	2.790	3.275	3.120

The cutoff radius was set to  $12.5 \text{ \AA}$  for all Lennard-Jones interactions. The long-range electrostatic interactions were handled using the Ewald-summation technique. The simulations were equilibrated for  $1.5 \times 10^7$  steps, then, the production run were carried out for  $1.5 \times 10^7$  steps.

Note that the unit of adsorption isotherm used in this study is the number of molecules, whereas that of the experiment is the volume of gas at STP per volume of ZIF-78 lattice, see Figure 3.3.



**Figure 3.3** Adsorption isotherm from the experiment [4].

The units of experimental values were converted to be number of molecules, in order to compare to the simulation results.

Figure 3.3 shows the experimental adsorption isotherms. It is found that the volume of gas at STP per volume of ZIF-78 lattice at 298 K 1 atm is 60 and the volume of the ZIF-78 ( $V_{ZIF-78}$ ) lattice of  $11540 \text{ \AA}^3$ , see Table 1.2.

$$\text{Thus, } \frac{V_{CO_2}(STP)}{V_{ZIF-78}} = 60 \quad (3.1)$$

$$\frac{V_{CO_2}(STP)}{11,514} = 60 \quad (3.2)$$

$$V_{CO_2}(STP) = 690,840 \text{ \AA}^3 = 6.91 \times 10^{-25} \text{ m}^3 = 6.91 \times 10^{-22} \text{ L} \quad (3.3)$$

In which the  $V_{CO_2}(STP)$  of  $6.91 \times 10^{-22} \text{ L}$  contains 18.57 moles  $CO_2$ .

### 3.3 Molecular dynamics simulations

MD simulations were performed to investigate the structural and dynamical properties. Here, the DREIDING force field parameters [30] were additionally used to describe the intramolecular interactions for the framework flexibility. The simulation box of ZIF-78 is

$52.2348 \times 52.2348 \times 38.9820 \text{ \AA}^3$  ( $2 \times 2 \times 2$  unit cells). The simulations were carried out at 298 K with the Berendsen thermostat.

The structure obtained from the XRD data was first optimized, then, the guest molecules,  $\text{CO}_2$  and  $\text{CH}_4$ , were inserted randomly. The cutoff radius of  $12.5 \text{ \AA}$ , and a time step of 1 fs were used. The simulation times are 0.5 ns for equilibration period and 1.5 ns for the production run. The trajectories were stored every 100 steps, and the radial distribution functions (RDFs) and dynamical diffusion coefficients ( $D_s$ ) were examined. The concentrations of guest molecules are varied on the same scale as experiment [4]. The  $\text{CO}_2$  and  $\text{CH}_4$  loadings per simulation box are 10, 65, 80, 150, 220 molecules and 5, 25, 45, 65 molecules, respectively. Our MD simulations were carried out for both single gas and binary gas systems. The concentration dependence of the self diffusion of guest molecules was investigated. For the binary mixture system, the concentration ratio of 1:1 (65  $\text{CO}_2$  molecules: 65  $\text{CH}_4$  molecules) was used. The diffusion selectivities obtained from single gas and binary gas have been compared.

### 3.4 Evaluations

#### 3.4.1 Radial distribution functions

RDFs were investigated to study the probability to find a particle of type  $j$  in a sphere of radius,  $r$ , around a particle of  $i$ . The atoms in ZIF-78 that can refer from Figure 3.4

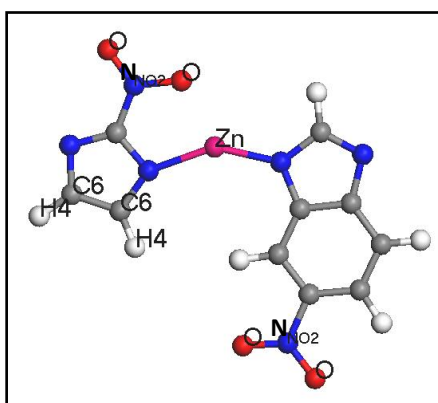


**Figure 3.4** Part of ZIF-78 structure and the atomic label.

The radial distribution functions can be calculated according to Eq. (2.10).

### 3.4.2 Probability density in $z$ direction

To see the adsorption site of the guest molecules, therefore the probability densities were analyzed. The ZIF-78 in each axis is shown in Figure 3.5

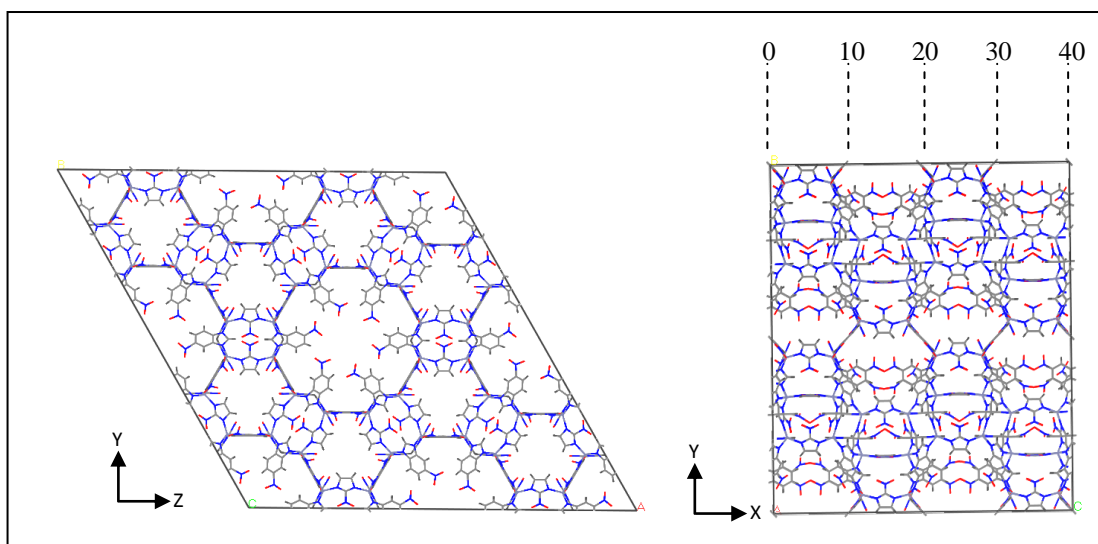


**Figure 3.5** The ZIF-78 in each axis.

The probability density is a dimensionless quantity, *e.g.* a value of 2 means that there are twice the number of atoms in the slab that if all atoms were distributed homogeneously across the system. The total number of atoms across all slabs is equal to the number of atoms in the entire system. So the sum of the probability densities of all slabs is equal to the number of slabs[40]. The probability densities can be calculated as follows Eq. (3.4).

$$\text{Probability densities } [\text{set}]_{\text{slab}} = [\text{set}]_{\text{slab}} / [\text{set}]_{\text{bulk}} \quad (3.4)$$

where

$$[\text{set}]_{\text{slab}} = N_{\text{slab}} / V_{\text{slab}}$$

$$[\text{set}]_{\text{bulk}} = N_{\text{bulk}} / V_{\text{bulk}}$$

### 3.4.3 Self-diffusion coefficient

The self-diffusion coefficient ( $D_s$ ) can be obtained from the linear fit to the mean square displacement (MSD) of guest molecules in ZIF-78. The MSDs were computed and averaged over the first 0.25 ps. The relation is explained by Einstein's equation (see Eq. (3.5))

$$MSD = 2\alpha D_s t + \beta \quad (3.5)$$

where,  $\alpha$  is the dimension, *i.e.*, 1, 2 and 3, and,  $\beta$  is the fitting parameter.

An example of MSD used for  $D_s$  calculation is shown in Figure 3.6

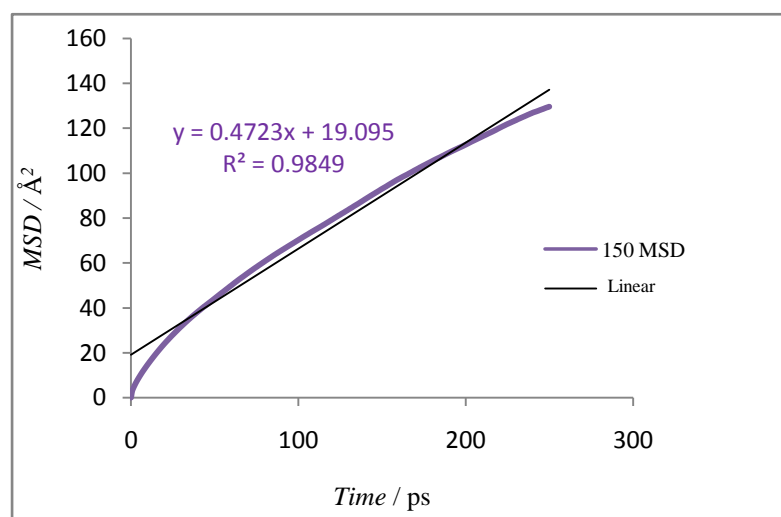


**Figure 3.6** An example of mean square displacement.

The MSD plot was fitted to the linear equation, see Figure 3.6. Here, the obtained slope was used to calculate the 3-dimensional  $D_s$  using Eq. (3.6).

$$D_s = \frac{m}{6} \quad (3.6)$$

This leads  $D_s$  to the  $0.0787 \text{ \AA}^2/\text{ps}$ .

### 3.4.4 Adsorption selectivity

The adsorption selectivity ( $S_{ads}$ ) for equimolar of CO<sub>2</sub> and CH<sub>4</sub> is expressed as

$$S_{ads}(CO_2/CH_4) = \frac{x_{CO_2}/x_{CH_4}}{y_{CO_2}/y_{CH_4}} \quad (3.7)$$

where  $x$  is the mole fraction of the adsorbed phase obtained from the GCMC simulations of mixture, and  $y$  the mole fraction of the bulk phase specified in term of pressure. All mixtures are equimolar in the bulk phase in this simulation.

Because all mixtures are equimolar in the bulk phase, thus, in this simulation only the  $x_{CO_2}$  and  $x_{CH_4}$  obtained from GCMC were used to calculate adsorption selectivity.

### 3.4.5 Diffusion selectivity

According to ref. [41] and ref. [42], the diffusion selectivity ( $S_{diff}$ ) of CO<sub>2</sub>/CH<sub>4</sub> can be calculated as follows

$$S_{diff}(CO_2/CH_4) = \frac{D_{CO_2,self}}{D_{CH_4,self}} \quad (3.8)$$

### 3.4.6 Membrane permeability

According to ref. [41] and ref. [42], membrane permeability of CO<sub>2</sub>/CH<sub>4</sub> mixture can be calculated from the adsorption and diffusion selectivities of CO<sub>2</sub>/CH<sub>4</sub> as follows

$$S_{membrane}(CO_2/CH_4) = S_{diff}(CO_2/CH_4) \times S_{ads}(CO_2/CH_4) \quad (3.9)$$



### 3.4.7 Knudsen selectivity

Knudsen selectivity can be calculated using Knudsen diffusion, which is the self-diffusion coefficient. Knudsen diffusion occurs when the mean free path is relatively long compared to the pore size, so the molecules collide frequently with the pore wall. Knudsen diffusion is dominant for pores that range in diameter between 2 and 50 nm.

Knudsen diffusion is described as

$$D_{i,Kn} = \frac{d_p}{3} \sqrt{\frac{8RT}{\pi M_i}} \quad (3.10)$$

where  $D_{i,Kn}$  is the Knudsen diffusion  
 $d_p$  is the pore diameters  
 $R$  is the gas constant  
 $T$  is Temperature  
 $M_i$  is the mass of molecule  $i$

Thus, the Knudsen selectivity of  $\text{CO}_2/\text{CH}_4$  mixture is

$$S_{\text{CO}_2/\text{CH}_4} = \frac{D_{\text{CO}_2,Kn}}{D_{\text{CH}_4,Kn}} = \sqrt{\frac{M_{\text{CH}_4}}{M_{\text{CO}_2}}} \quad (3.11)$$

## CHAPTER IV

### RESULTS AND DISCUSSION

#### 4.1 Validation of guest-host interaction parameter

The GCMC algorithm has been used to validate the force field parameters for guest molecules in the ZIF-78 system. The adsorption isotherms of CO<sub>2</sub> and CH<sub>4</sub> in ZIF-78 are shown in Figure 4.1. The adsorption isotherm of CH<sub>4</sub> obtained from our simulations is in agreement with that of experiment. For the adsorption isotherm of CO<sub>2</sub>, the best force field parameters that one can find from the literatures have been taken. However, the simulated adsorption isotherm of CO<sub>2</sub> is higher than that from the experiment [4]. It is known that the procedure to develop the force field parameter is quite complicated. We thus decided to use this set of force field parameters for MD of CO<sub>2</sub> in ZIF-78 in this work.

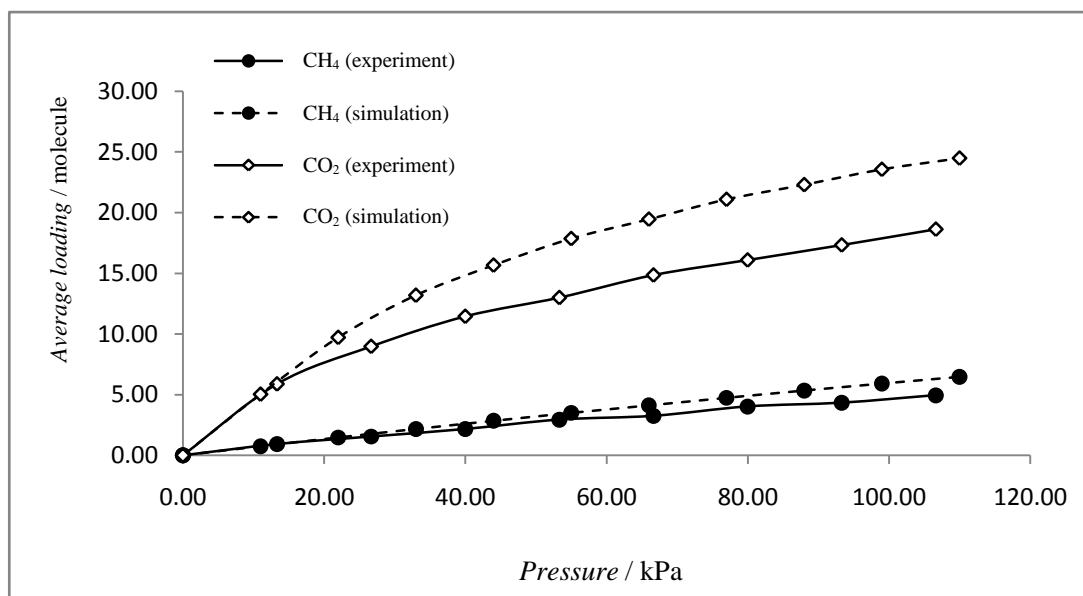


**Figure 4.1** The calculated adsorption isotherm at 298 K for CO<sub>2</sub> and CH<sub>4</sub> in comparison to that obtained from the experiment [4].

## 4.2 Structure of CO<sub>2</sub> and CH<sub>4</sub> in ZIF-78 lattice

### 4.2.1 Radial distribution functions, RDFs

To obtain structural data of CO<sub>2</sub> and CH<sub>4</sub> absorbed in ZIF-78 from MD, the radial distribution function (RDF),  $g_{ij}(r)$  which is the probability density to find a particle  $j$  at the distance  $r$ , around a particle  $i$ , were calculated. In this work,  $i$  represent the atom in ZIF-78 lattice (Figure 4.2) whereas  $j$  represents the C and O atoms of CO<sub>2</sub>, and, the C and H atoms of CH<sub>4</sub>. For better understanding, only important RDFs were shown.

The RDFs from the atom in ZIF-78 to C and O atoms of CO<sub>2</sub> are shown in Figure 4.3a-4.3b, respectively. The RDFs for various concentrations of guest molecule from C and O atoms of CO<sub>2</sub> to O (Figure 4.3c-4.3d) and Zn (Figure 4.3e-4.3f) atoms of ZIF-78 are shown.

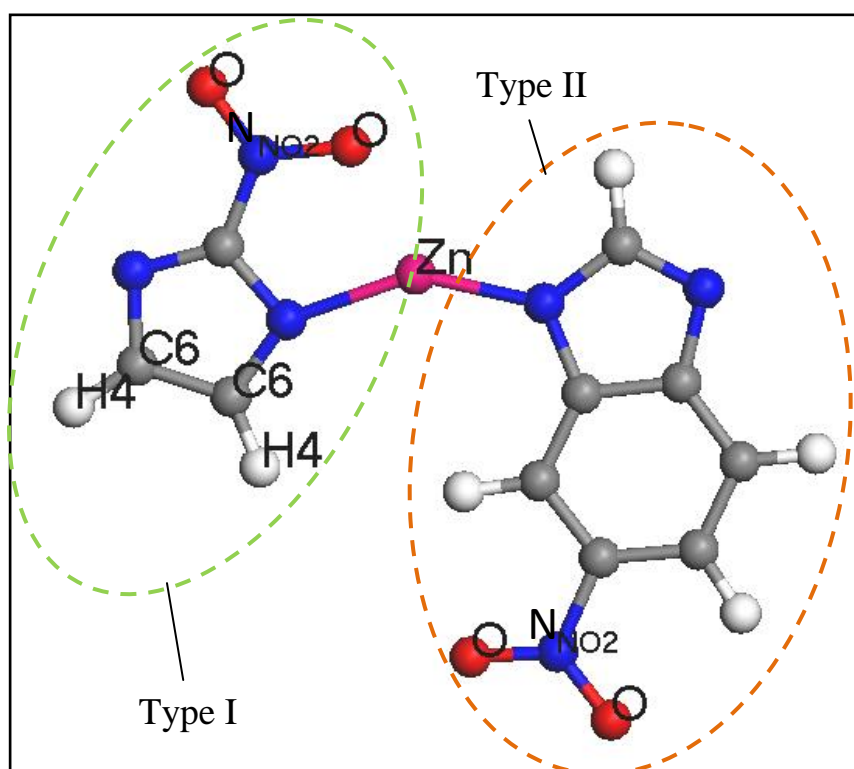


**Figure 4.2** Two types of linker, *i.e.*, nitroimidazolate (Type I) and nitrobenzimidazolate (Type II) coordinated to Zn ion are shown. The labels of atom type are also given.

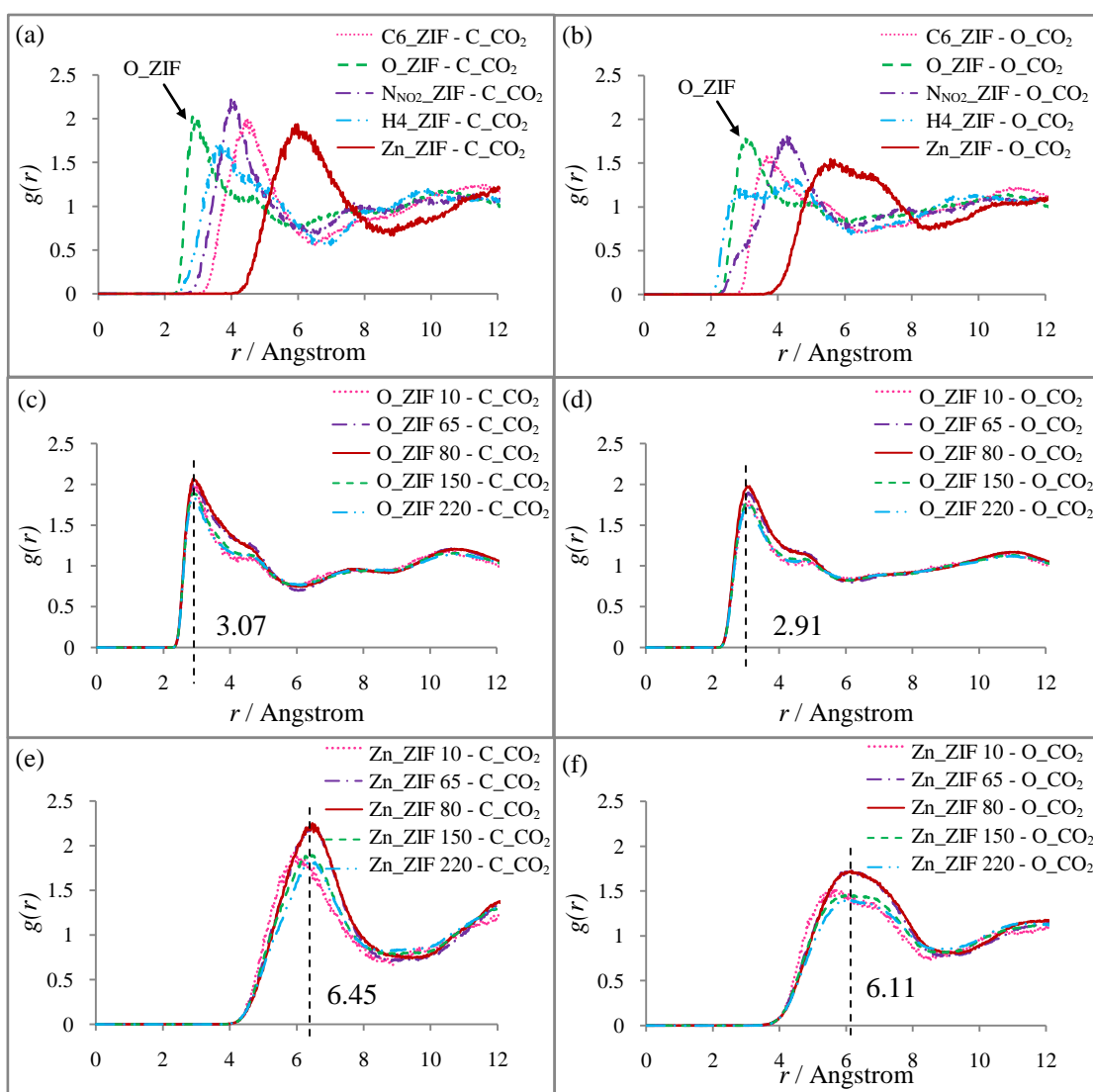


**Figure 4.3** RDFs from ZIF-78 to atoms of  $\text{CO}_2$ ,  $i_{\text{ZIF}} - j_{\text{CO}_2}$  where  $i$  are the atoms of ZIF-78 (see Figure 4.2 for label) and  $j$  represents the atoms of  $\text{CO}_2$ .

The characteristics of  $\text{CO}_2$  adsorption in ZIF-78 can be understood from Figure 4.3. For all atoms of lattice with all  $\text{CO}_2$  loading, the first sharp peaks of O in ZIF-78 centered at 3.07 Å (Figure 4.3c) and 2.91 Å (Figure 4.3d) observed for C and O atoms of  $\text{CO}_2$ , respectively. In case of  $\text{Zn\_ZIF-C\_CO}_2$  and  $\text{Zn\_ZIF-O\_CO}_2$  (Figure 4.3e and 4.3f) RDFs, the peaks are centered at 6.45 Å for C and 6.11 Å for O of  $\text{CO}_2$ . It indicates that  $\text{CO}_2$  adsorbs firmly to the O of  $-\text{NO}_2$  group in which the most probable distances from O of  $-\text{NO}_2$  group to C and O atoms of  $\text{CO}_2$  are 3.07 Å and 2.91 Å, respectively.

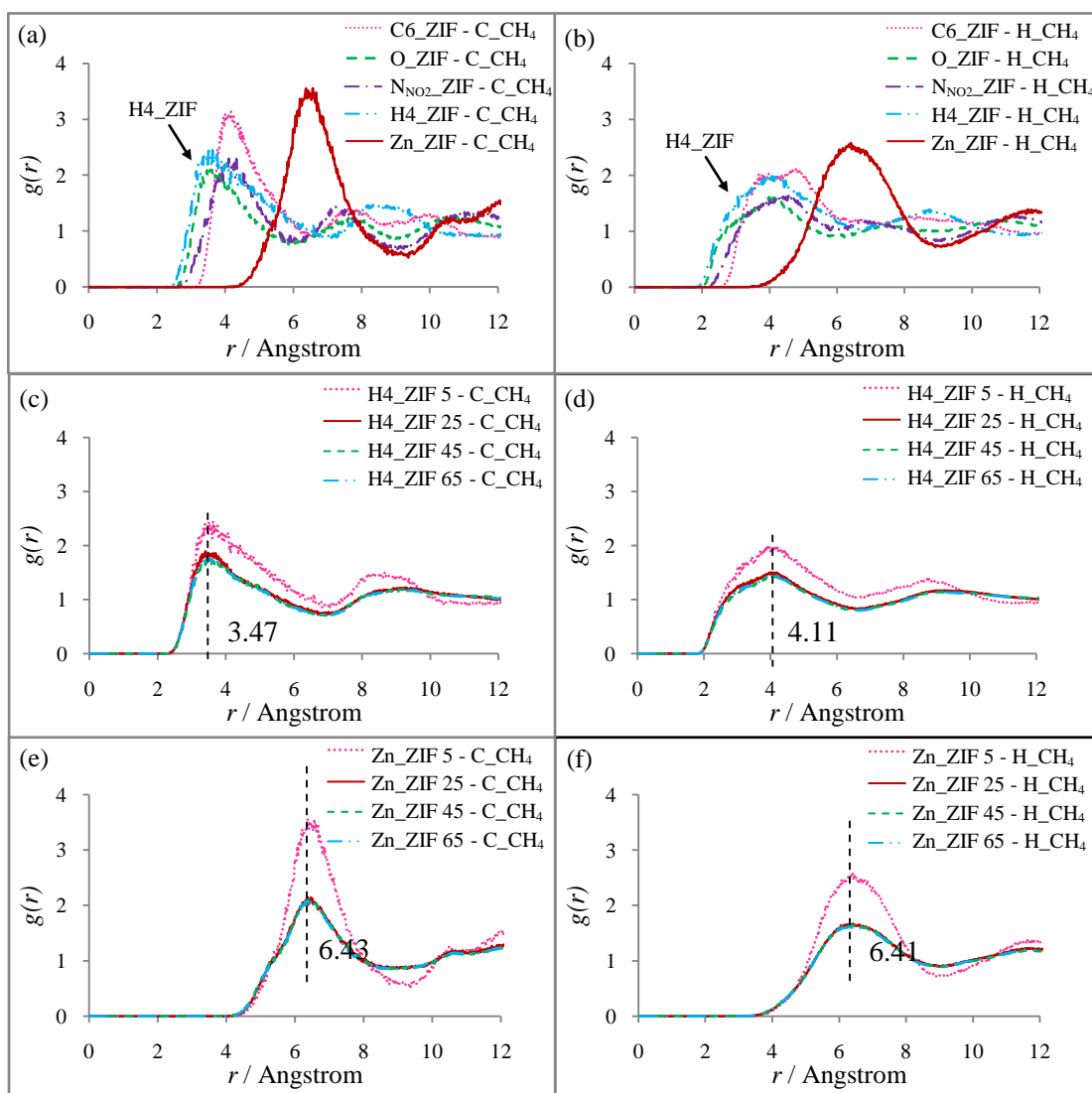


**Figure 4.4** RDFs from ZIF-78 to atoms of  $\text{CH}_4$ ,  $i_{\text{ZIF}} - j_{\text{CH}_4}$ , where  $i$  are the atoms of ZIF-78 (see Figure 4.2 for label) and  $j$  represents the atoms of  $\text{CH}_4$ .

With four different loading of  $\text{CH}_4$ , the RDFs show the first sharp peak centered at 3.47 Å for  $\text{H4\_ZIF} - \text{C\_CH}_4$  (Figure 4.4c) while the farthest distinct peak is 6.43 Å for  $\text{Zn\_ZIF} - \text{C\_CH}_4$  (Figure 4.4e). From the results, it indicates that H atoms of nitroimidazole group (H4 in Figure 4.2) are the preferred adsorption sites for  $\text{CH}_4$ . It is worth to note that, the broaden of all peaks from the atoms of ZIF-78 to H atoms of  $\text{CH}_4$  (Figures. 4.4b, 4.4d and 4.4f) is due to free orientation of the four H atoms in  $\text{CH}_4$  molecule.

In addition, the concentration dependence does not detect in case of  $\text{CO}_2$  (Figures 4.3c-f) but it is clearly observed for  $\text{CH}_4$  (Figures 4.4c-f). With increasing loading of  $\text{CH}_4$ , the peak

intensities of RDFs decrease significantly. It implies the  $\text{CH}_4$  molecule does not adsorb firmly at H4 of nitroimidazolate linker – short resident time.

Figure 4.5 visualized the adsorption sites of guest molecules in ZIF-78.

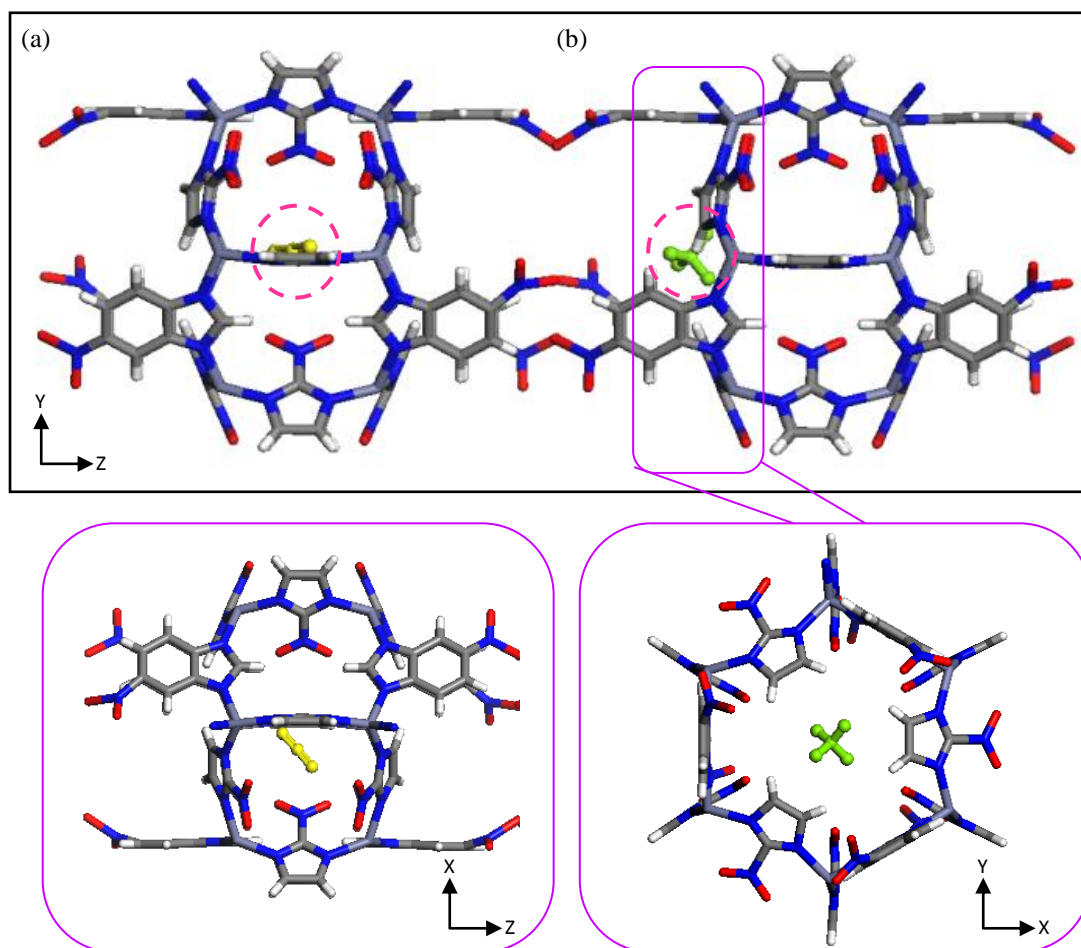


**Figure 4.5** Schematic of the adsorption sites of (a)  $\text{CO}_2$  (yellow) and (b)  $\text{CH}_4$  (green) in ZIF-78.

To understand in more details, we thus calculated the probability density of guest molecules in ZIF-78. This will be discussed in the next section.

#### 4.2.2 Probability density

The probability densities to find the guest molecules in  $z$  direction of ZIF-78, were calculated and shown in Figure 4.6.

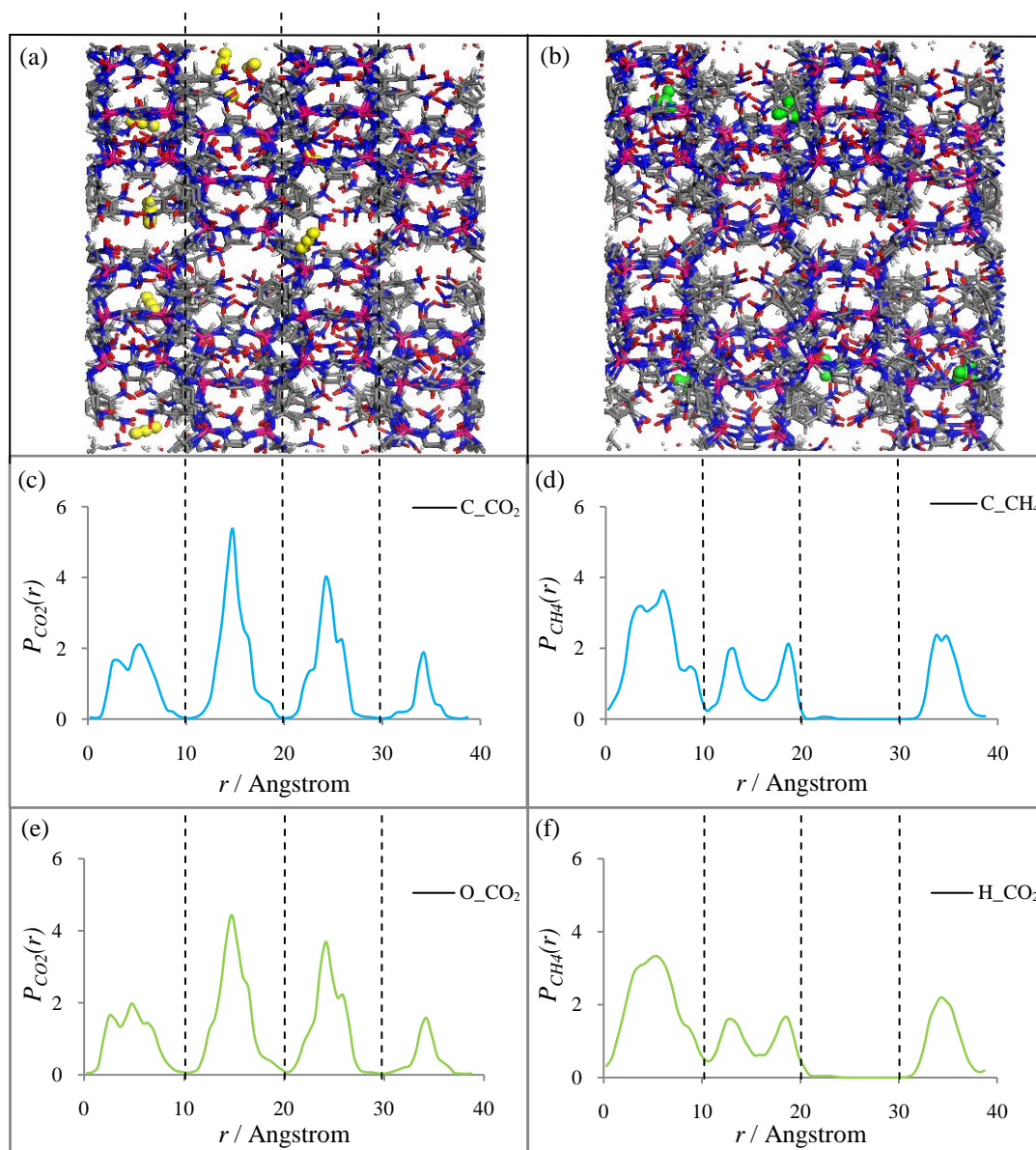


**Figure 4.6** The snapshot of (a) 10 molecules of CO<sub>2</sub> and (b) 5 molecules of CH<sub>4</sub> in ZIF-78, as well as probabilities density in z-direction of (c) 10 molecules of C atom of CO<sub>2</sub>, (d) 5 molecules of C atom of CH<sub>4</sub>, (e) 10 molecules of O atom of CO<sub>2</sub>, (f) 5 molecules of H atom of CH<sub>4</sub>. Here, the dash line show the edges of lattice channel.

The density plots of the guest molecules located in z-direction of ZIF-78 show clearly that the CO<sub>2</sub> molecules (Figures 4.6c and e) prefer to absorb at the middle of the channel. On the other hand, the CH<sub>4</sub> molecules (Figures 4.6d and f) are mostly observed near the edge of the channel. This can be explained by the polarity of the contributed atoms in lattice. The edge of

lattice channel comprises of many non-polar atoms, especially, C and H atoms of nitroimidazolate linker which is preferred by the non-polar  $\text{CH}_4$  molecule, whereas, the polar  $\text{CO}_2$  molecules prefer the polar site which are the nitro groups established at the middle of channel.

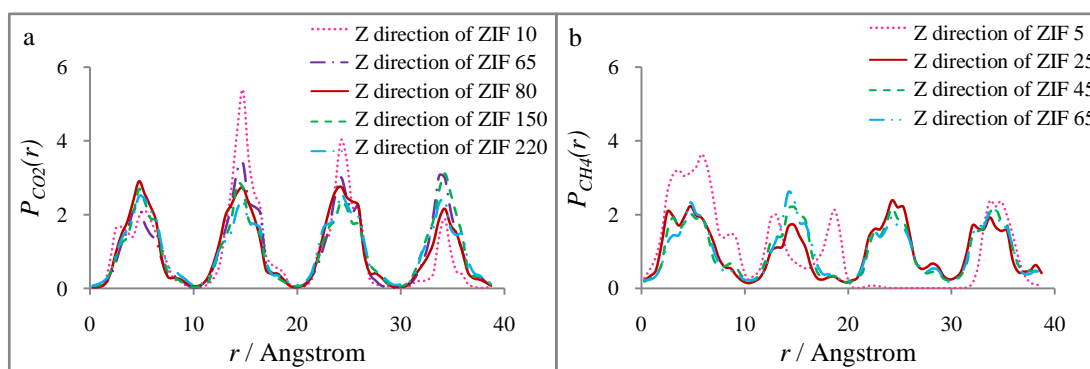


**Figure 4.7** The probability density in  $z$ -direction for (a) C atom of  $\text{CO}_2$  and (b) C atom of  $\text{CH}_4$  for various concentrations.

With increasing guest loading, the  $\text{CO}_2$  molecules remain at the same adsorption site, *i.e.*, nitro group whereas the  $\text{CH}_4$  molecules are additionally detected at the middle of the channel.

### 4.3 Self diffusivity

The mean square displacements (MSD) of  $\text{CO}_2$  and  $\text{CH}_4$  molecules at concentrations of 10, 65, 80, 150 and 220 molecules per simulation box, have been computed.

The MSD of guest molecules are computed over 250 ps of time and averaged over the first 250 ps of a 500 ps trajectory.



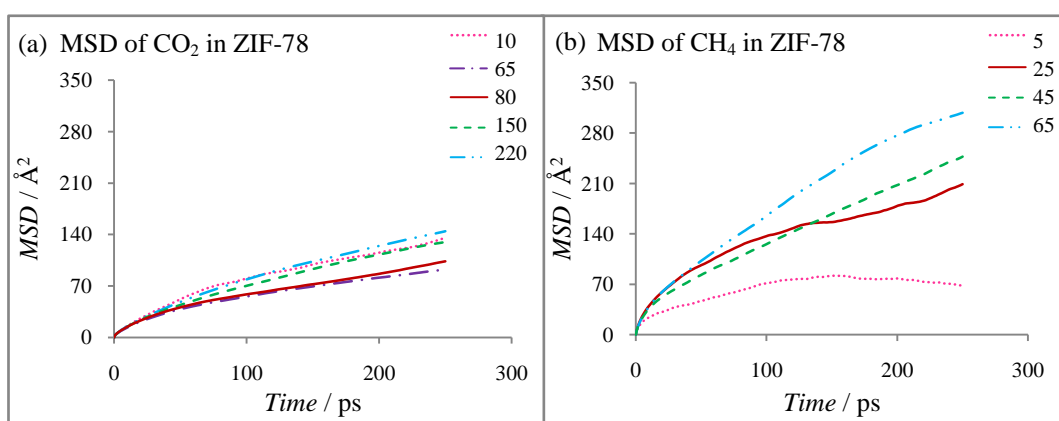


**Figure 4.8** The calculated MSD with loading dependence of (a) CO<sub>2</sub> and (b) CH<sub>4</sub> in ZIF-78.

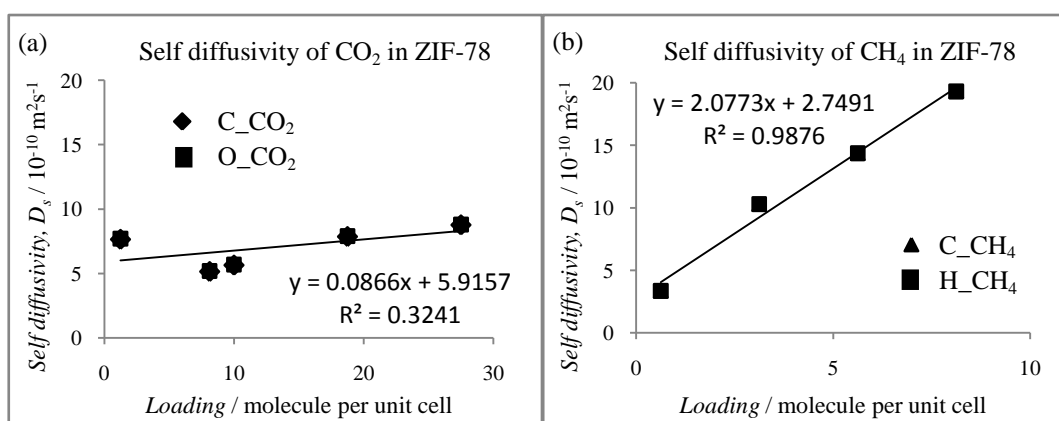


**Figure 4.9** The self diffusivity with loading dependence of (a) CO<sub>2</sub> and (b) CH<sub>4</sub> in ZIF-78.

The self diffusivity of CO<sub>2</sub> and CH<sub>4</sub> molecules in ZIF-78 can be described by the self diffusion coefficient,  $D_s$ . The  $D_s$  values were obtained from the linear fit to the mean-square displacement (see Figure 4.8, and Eq. (3.5)). The calculated  $D_s$  with guest loading are plotted in Figure. 4.9a and 4.9b for CO<sub>2</sub> and CH<sub>4</sub>, respectively. It is clearly seen that the  $D_s$  values of CH<sub>4</sub> significantly increase with increasing loading, whereas the  $D_s$  values of CO<sub>2</sub> do not depend very much on loading. This significant increasing of  $D_s$  can be resulted from the rapid decrease of RDFs for H4\_ZIF - C\_CH<sub>4</sub>. The CH<sub>4</sub> molecule does not adsorb firmly at the adsorption site. They can easily move in the lattice-increase of  $D_s$ .

#### 4.4 Adsorption selectivity

The adsorption selectivity ( $S_{ads}$ ) of  $\text{CO}_2$  from  $\text{CO}_2/\text{CH}_4$  mixture can be calculated using Eq. (3.7), in which, the ratio of  $y_{\text{CO}_2}/y_{\text{CH}_4}$  is equal to 1.

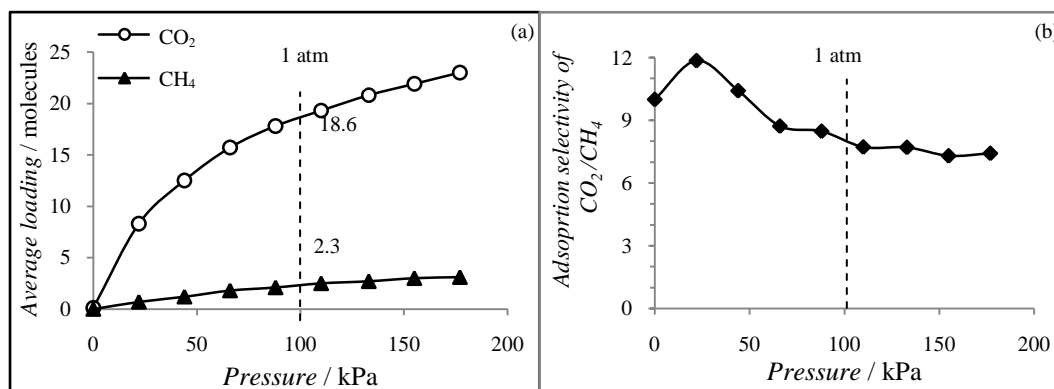


**Figure 4.10** (a) Adsorption isotherm of  $\text{CO}_2$  and  $\text{CH}_4$  calculated from GCMC simulation of equimolar mixture at 298 K, as well as, (b) the corresponding adsorption selectivity calculated from Eq. (3.7) at different pressure.

Adsorption isotherm of  $\text{CO}_2/\text{CH}_4$  mixture with equimolar calculated from GCMC simulation and corresponding adsorption selectivity of  $\text{CO}_2/\text{CH}_4$  at 298 K are shown in Figure 4.10a and 4.10b, respectively. From both adsorption isotherm, it clearly seen that ZIF-78 prefers to adsorb the  $\text{CO}_2$  than  $\text{CH}_4$ . At 1 atm (101.3 kPa),  $\text{CO}_2$  can adsorb at about 18.6 molecules whereas it is about 2.3 molecules in case of  $\text{CH}_4$ . Figure 4.10b shows the adsorption selectivity that calculated from the adsorption isotherm of  $\text{CO}_2/\text{CH}_4$  mixture (see Figure 4.10a) using Eq. (3.7). It found that all the values of adsorption selectivity are greater than 1 which indicate that ZIF-78 is selective for  $\text{CO}_2$  than  $\text{CH}_4$  – used as separator for  $\text{CO}_2$  from  $\text{CO}_2/\text{CH}_4$  mixture. It is worth to note that the maximum of  $S_{abs}$  at 25 kPa is cause by the rapid increase of adsorption isotherm of  $\text{CO}_2$  whereas the  $\text{CH}_4$  is adsorbed gradually.

#### 4.5 Diffusion selectivity

The diffusion selectivity ( $S_{diff}$ ) of CO<sub>2</sub> from CH<sub>4</sub> can be computed using Eq. (3.8) as mentioned in chapter 3

The calculated diffusion selectivities of CO<sub>2</sub> at different CO<sub>2</sub>/CH<sub>4</sub> ratios are shown in Table 4.1a (see also Eq. (3.8)). The  $S_{diff}$  values for the single gas systems calculated from the single gas system have been compared with the value obtained from the binary gas simulation runs. Note that the simulation of the binary gas system was carried out at only the ratio of 1:1.

**Table 4.1** The calculated diffusion selectivity of CO<sub>2</sub> in CO<sub>2</sub>/CH<sub>4</sub> mixture at different ratios.

A)	
Single gas	
$S_{diff}(CO_2/CH_4)$	
@ 1 : 0.5 (10:5) = 2.2765	
@ 1 : 1.0 (10:10) = 2.2774	
@ 1 : 2.5 (10:25) = 0.7434	
@ 1 : 4.5 (10:45) = 0.5329	
@ 1 : 6.5 (10:65) = 0.3963	
B)	
Single gas	Binary gas
$S_{diff}(CO_2/CH_4)$	$S_{diff}(CO_2/CH_4)$
@ 1 : 1 (65:65) = 0.2668	@ 1 : 1 (65:65) = 0.2925

At 298 K,  $S_{diff}$  of CO<sub>2</sub> from 1:1 of CO<sub>2</sub>/CH<sub>4</sub> mixture, which is obtained from the single gas simulation is 2.2774, see Table 4.1a. The  $S_{diff}$  decrease with increasing CH<sub>4</sub> loading. For the  $S_{diff}$  of CO<sub>2</sub> from 1:1 of CO<sub>2</sub>/CH<sub>4</sub> mixture, which obtained from single gas and binary gas simulations are 0.2668, 0.2925, respectively. It indicates that the  $S_{diff}$  from both simulations are close to each other. Therefore, both methods can be comparable.

Moreover, the Knudsen selectivity has been also calculated using the Eq. (3.11) (see chapter 3) where  $M_{CH_4}$  and  $M_{CO_2}$  are the molecular mass of CH<sub>4</sub> and CO<sub>2</sub>, respectively. The selectivity value predicted from the Knudsen formula for CO<sub>2</sub>/CH<sub>4</sub> is found to be 0.014, which is

significantly different from the diffusion selectivity. This means that the size, shape or other properties are more important than the molecular mass, and can play a role in this system.

#### 4.6 Membrane permeability

To calculate membrane permeability of  $\text{CO}_2$  from  $\text{CO}_2/\text{CH}_4$  mixture, both  $S_{ads}$  and  $S_{diff}$  are required and can be obtained using Eq. (3.9).

Membrane selectivity of  $\text{CO}_2$  from  $\text{CH}_4$  at vacuum, 298 K is equal 2.16. As mentioned that the values calculated from Eq. (3.9) are greater than 1, showing that this ZIF material is selective for component  $\text{CO}_2$  in  $\text{CO}_2/\text{CH}_4$  mixture. Hence, membrane base separation can also use to separate  $\text{CO}_2$  from  $\text{CH}_4$ .

In conclusion, adsorption selectivity, diffusion selectivity, and membrane permeability of ZIF-78 for  $\text{CO}_2/\text{CH}_4$  were shown in Figure 4.11.

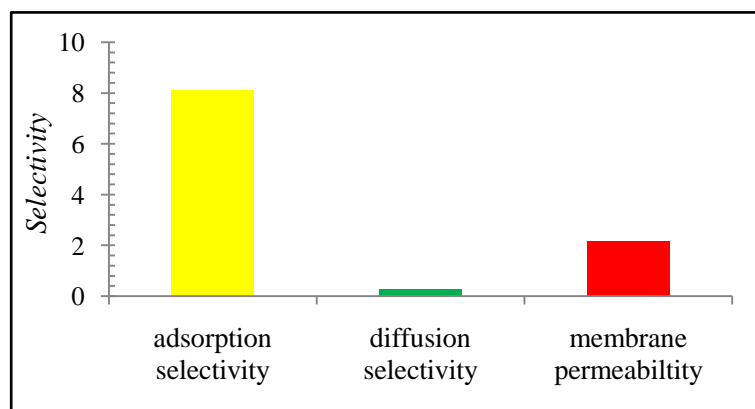


**Figure 4.11** Adsorption selectivity, diffusion selectivity, and membrane permeability of ZIF-78 for  $\text{CO}_2/\text{CH}_4$ .

The adsorption selectivity, diffusion selectivity, and corresponding membrane permeability of ZIF-78 for  $\text{CO}_2/\text{CH}_4$  mixture are shown in Figure 4.11. It is found that the adsorption selectivity is high and the value of diffusion selectivity quite low, which indicates that the adsorption selectivity play the importance role in membrane based separation.

## CHAPTER V

### CONCLUSIONS

Two computer simulation techniques have been used to understand the molecular insight into adsorption and diffusion phenomena of CO<sub>2</sub> and CH<sub>4</sub> in ZIF-78. GCMC was conducted to obtain the adsorption isotherm of the guest molecules in ZIF-78 in order to validate the force field parameter used. The simulated adsorption isotherm of CH<sub>4</sub> in ZIF-78 agrees with the experiment, indicating the quality of the force field. The adsorption isotherm of CO<sub>2</sub> in ZIF-78 is found to be somehow different from the experiment, however, this is the best set of force field from the literatures.

The validated force field parameters were applied to MD simulations to obtain the structural and dynamic properties of guest molecules in ZIF-78 in terms of radial distribution functions (RDFs) and probability density as well as self-diffusivity ( $D_s$ ), respectively. The CO<sub>2</sub> molecules prefer to adsorb at the O atoms of -NO<sub>2</sub> group located at the middle of ZIF-78 channel whereas the CH<sub>4</sub> molecules were mostly observed at the edge of lattice channel located at the H4 of nIm linker. The  $D_s$  of CH<sub>4</sub> is concentration dependence while it does not in case of CO<sub>2</sub>.

To understand the separation of CO<sub>2</sub> by ZIF-78 material, two kinds of CO<sub>2</sub> selectivity have been determined. First, the adsorption selectivity ( $S_{ads}$ ) calculated from the adsorption isotherm of equimolar of CO<sub>2</sub>/CH<sub>4</sub> binary mixtures is about 8.08 at 1 atm (101.3 kPa) which indicates the high efficiency of equilibrium-based separation of CO<sub>2</sub> by ZIF-78. Secondly, the diffusion selectivity ( $S_{diff}$ ) computed from the ratio between the self diffusivity of each gas is found to be about 0.3. From both selectivity values, the membrane permeability was calculated. It is clearly seen that the adsorption selectivity dominates the membrane permeability. On the other word, it plays the important role in membrane-based separation.

For our further work, the force field parameters for CO<sub>2</sub> in ZIF-78 should be developed to have an agreement with experiment. Moreover, the diffusion selectivity of CO<sub>2</sub>/CH<sub>4</sub> mixture which obtained from binary gas simulation should be calculated for various CO<sub>2</sub>:CH<sub>4</sub> ratios, in order compare to the one obtained from single gas simulation.

## REFERENCE

- [1] Tagliabue M.; Farrusseng D.; Valencia S.; Aguado S.; Ravon U.; Rizzo C.; Corma A. and Mirodatos C. Natural gas treating by selective adsorption: material science and chemical engineering interplay. *Chem. Eng. J.* 155 (2009): 553–566.
- [2] Park K. S.; Ni Z.; Cote A. P.; Choi J. Y.; Hueang R.; Uribe-Romo F. J.; Chae H. K.; O’Keeffe M. and Yaghi O. M. Exceptional chemical and thermal stability of zeolitic imidazolate frameworks. *PNAS* 103 (2006): 10186-10191.
- [3] Hayashi H.; Côté A. P.; Furukawa H.; O’Keeffe M. and Yaghi O. M. Zeolite a imidazolate frameworks. *Nat. Mater.* 6(2007): 501-506.
- [4] Banerjee R.; Furukawa H.; Britt D.; Knobler C.; O’Keeffe M. and Yaghi O. M.; Control of pore size and functionality in isorecticular zeolitic imidazolate frameworks and their carbon dioxide selective capture properties *J. Am. Chem. Soc.* 131(2009): 3875-3877.
- [5] Phan A.; Doonan C. J.; Uribe-Romo F. J.; Knobler C. B.; O’Keeffe M. and Yaghi O. M. Synthesis, structure, and carbon dioxide capture properties of zeolitic imidazolate frameworks *Acc. Chem. Res.* 43(2010): 58–67.
- [6] Kunchana Bunyakiat and Chawalit Ngamcharussrivichai. *Natural gas technology*. Chulalongkorn University Press, 2008
- [7] Chen Y.; Liu Q. L.; Zhu A. M.; Zhang Q. G. and Wu J. Y. Molecular simulation of CO<sub>2</sub>/CH<sub>4</sub> permeabilities in polyamide–imide isomers *J. Mem. Sci.* 348(2010): 204–212.
- [8] Yaghi O. M. and Goddard III W. A. A joint theory and experimental project in the high- throughput synthesis and testing of porous COF and ZIF Materials for on- board vehicular hydrogen storage [slides]. Department of chemistry center for reticular chemistry UCLA and Department of chemistry, materials science and applied physics caltech, 2009

- [9] Tran U. P. N.; Le K. K. A.; and Phan N. T. S. Expanding applications of metal-organic frameworks: zeolite imidazolate framework ZIF-8 as an efficient heterogeneous catalyst for the knoevenagel reaction. *ACS Catal.* 1(2011): 120–127.
- [10] Benerjee R.; Pahn A.; Wang, B.; Knobler C.; Furukawa H.; O’Keeffe M.; Yaghi O. M. High-throughput synthesis of zeolitic imidazolate frameworks and application to CO<sub>2</sub> capture. *Science* 319(2008): 939-943.
- [11] Wang B.; Côté A. P.; Furukawa H.; O’Keeffe M. and Yaghi, O. M. Colossal cages in zeolitic imidazolate frameworks as selective carbon dioxide reservoirs *Nature* 453(2008): 207-212.
- [12] Zhou W.; Wu H.; Hartman M. R. and Yildirim T. Hydrogen and methane adsorption in metal-organic frameworks: a high-pressure volumetric study *J. Phys.Chem. C* 111(2007): 16131–16137.
- [13] Wu H.; Zhou W. and Yildirim T. Hydrogen storage in a prototypical zeolitic imidazolate framework-8. *J. Am. Chem. Soc.* 129(2007): 5314-5315.
- [14] CBC News article New materials can selectively capture CO<sub>2</sub>, scientists say published February 15, 2008
- [15] Venna S. R. and Carreon M. A. Highly permeable zeolite imidazolate framework-8 membranes for CO<sub>2</sub>/CH<sub>4</sub> separation *J. Am. Chem. Soc.* 132(2010): 76–78.
- [16] Hertäg L.; Bux H.; Caro J.; Chmelik C.; Remsungnen T.; Knauth M. and Fritzsche S. Diffusion of CH<sub>4</sub> and H<sub>2</sub> in ZIF-8. in press.
- [17] Ordoñez M. J. C.; Balkus Jr K. J.; Ferraris J. P. and Musselman I. H. Molecular sieving realized with ZIF-8/matrimid mixed-matrix membranes. *J. Mem. Sci.* 361(2010): 28–37.
- [18] Liu D.; Zheng C.; Yang Q. and Zhong C. Understanding the adsorption and diffusion of carbon dioxide in zeolitic imidazolate frameworks: a molecular simulation study *J. Phys. Chem. C* 113(2009): 5004–5009.

- [19] Sirjoosingh A.; Alavi S. and Woo T. K. Grand-canonical monte carlo and molecular-dynamics simulations of carbon-dioxide and carbon-monoxide adsorption in zeolitic imidazolate framework materials *J. Phys. Chem. C* 114(2010): 2171–2178.
- [20] Rankin R. B.; Liu J.; Kulkarni A. D. and Johnson J. K. Adsorption and diffusion of light gases in ZIF-68 and ZIF-70: a simulation study. *J. Phys. Chem. C* 113(2009): 16906–16914.
- [21] Hou X.-J. and Li H. Unraveling the high uptake and selectivity of CO<sub>2</sub> in the zeolitic imidazolate frameworks ZIF-68 and ZIF-69. *J. Phys. Chem. C* 114(2010): 13501–13508.
- [22] Liu B. and Smit B. Molecular simulation studies of separation of CO<sub>2</sub>/N<sub>2</sub>, CO<sub>2</sub>/CH<sub>4</sub>, and CH<sub>4</sub>/N<sub>2</sub> by ZIFs. *J. Phys. Chem. C* 114(2010): 8515–8522.
- [23] Keskin S. Atomistic simulations for adsorption, diffusion, and separation of gas mixtures in zeolite imidazolate frameworks *J. Phys. Chem. C* 115(2011): 800–807.
- [24] Ropero F. R., Application of molecular simulation techniques to the design of nano systems, Doctoral dissertation, Department D'enginyeria química, Universitat Politècnica de catalunya, 2009
- [25] Supot Hannongbua, Computer Simulation: Monte Carlo Method (slides). Chulalongkorn University, 2002
- [26] Liu B. Molecular simulation studies of adsorption and diffusion : phenomena of gases in Porous materials. Doctoral dissertation, Faculty of Science University of Amsterdam, 2008
- [27] Alder B.J. and Wainwright T.E. Phase transition for a hard sphere system. *J. Chem. Phys.* 27(1957): 1208–1209.
- [28] Pornthep Sompornpisut, Molecular dynamic (MD) simulation (slides). Computational chemistry unit cell, Chulalongkorn University, 2010
- [29] Casewit C. J.; Colwell K. S. and Rappe' A. K. Application of a universal force field to organic molecules. *J. Am. Chem. Soc.* 114(1992): 10024–10035
- [30] Mayo S. L; Olafson B. D. and Goddard III W. A. DREIDING: A Generic Force Field for Molecular Simulations. *J. Phys. Chem.* 94(1990): 8897-8909
- [31] Supot Hannongbua, Molecular Dynamics Method (slides). Chulalongkorn University, 2002



- [32] Swope W. C.; Andersen H. C.; Berens P. H. and Wilson K. R. A computer simulation method for the calculation of equilibrium constants for the formation of physical clusters of molecules: application to small water clusters. J. Chem. Phys. 76(1982): 637-649
- [33] Hockney R. W. and Eastwood J. W. Computer simulations using particles. Adam Hilger, Bristol, 1988.
- [34] D. Beeman, Some multistep methods for use in molecular dynamics calculations, J Comp. Phys. 20(1976): 130-139
- [35] Tanawut Ploymeerusmee, Metal organic frameworks MOF-5 as carbon dioxide storage studied by computational chemistry methos. Master's thesis, Field of Petrochemistry and Polymer Science, Faculty of Science, Chulalongkorn University, 2008.
- [36] Martin M. G. and Siepmann J. I. Transferable Potentials for Phase Equilibria. 1. United-Atom Description of *n*-Alkanes, J. Phys. Chem. B 102(1998): 2569-2577
- [37] Allen M. P. Introduction to Molecular Dynamics Simulation John von Neumann Institute for Computing, J ulich, NIC Series, 2004
- [38] Sánchez C, Computational studies on the structure and dynamic of bioactive peptides. Doctoral dissertation, Chemical engineer Department, Barcelona, September 2003
- [39] Acceleys Software Inc., Forcite Training Manual (slides). Accelrys Software Inc., San Diego, CA, 2008
- [40] Acceleys Software Inc., Materials Studio, 5.0V, San Diego: Accelrys Software Inc., 2009.
- [41] Graaf J. M.; Kapteijn F. and Moulijn J. A., Modeling permeation of binary mixtures through zeolitic membranes. AIChE J. 45(1999): 497-511
- [42] Krishna R. and Baten J. M. Influence of adsorption on the diffusion selectivity for mixture permeation across mesoporous membranes J. Mem. Sci. 369(2011): 545-549.

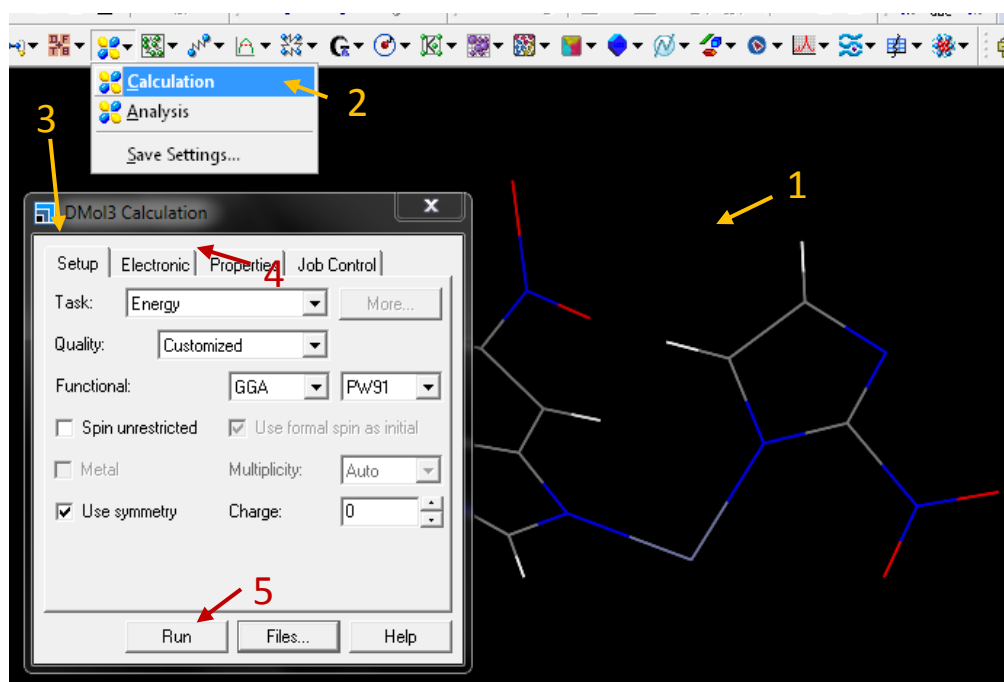
## **APPENDICES**

## **APPENDIX A**

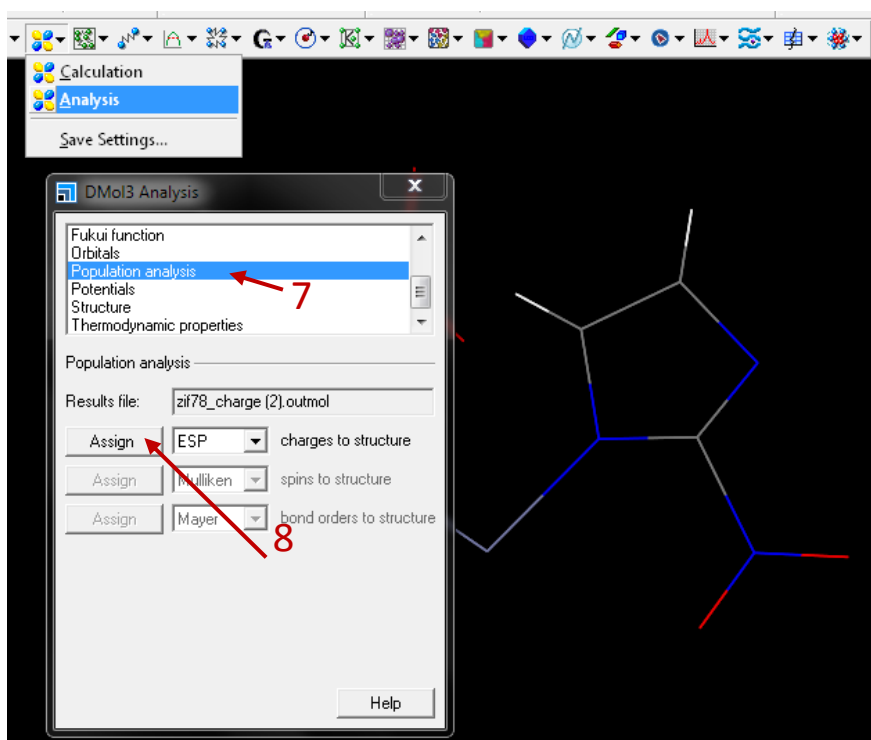
Module used in Material Studio Program for this thesis.

## 1. How to calculate charges.

The partial charges are obtain from the procedure as follow



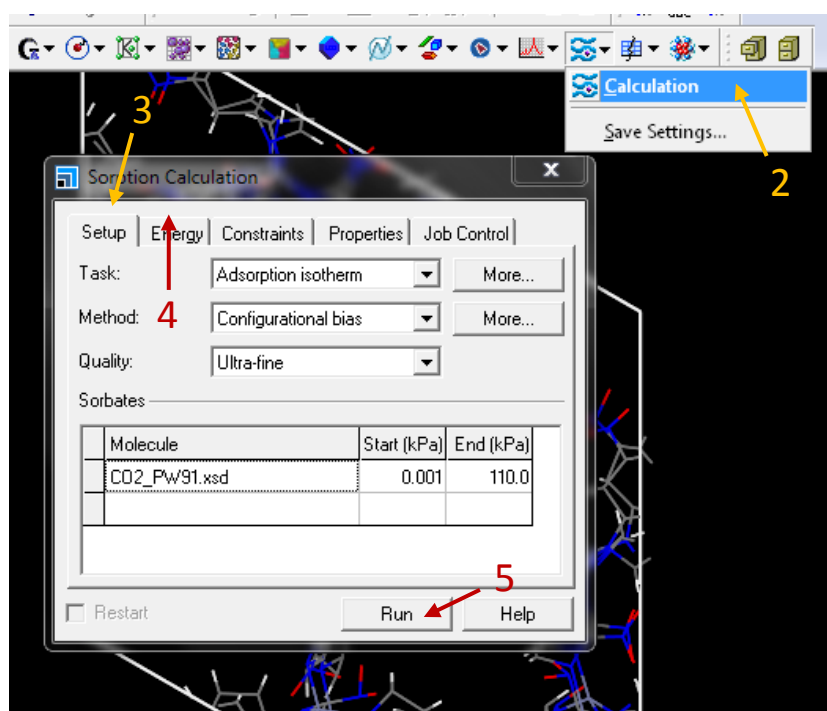
- i. Open the lattice structure that was cut to be a repeating unit.
- ii. Click calculates on *Dmol<sup>3</sup>* module.
- iii. In Setup bar choose Task, Quality and Functional to be Energy, Customized and GGA and PW91
- iv. In the Electronic bar choose basis set to be DND and in the Properties bar click on Population analysis.
- v. In the Job control bar click on Run to calculate the charge.



- vi. Open the result (.xsd)
- vii. Click analysis on *Dmol<sup>3</sup>* module.
- viii. Select the Population analysis and select the ESP from dropdown list and click on Assign to obtain charge.

## 2. How to obtain adsorption isotherm

Step of using the *Sorption* module to calculation the adsorption isotherm from the GCMC simulation follow

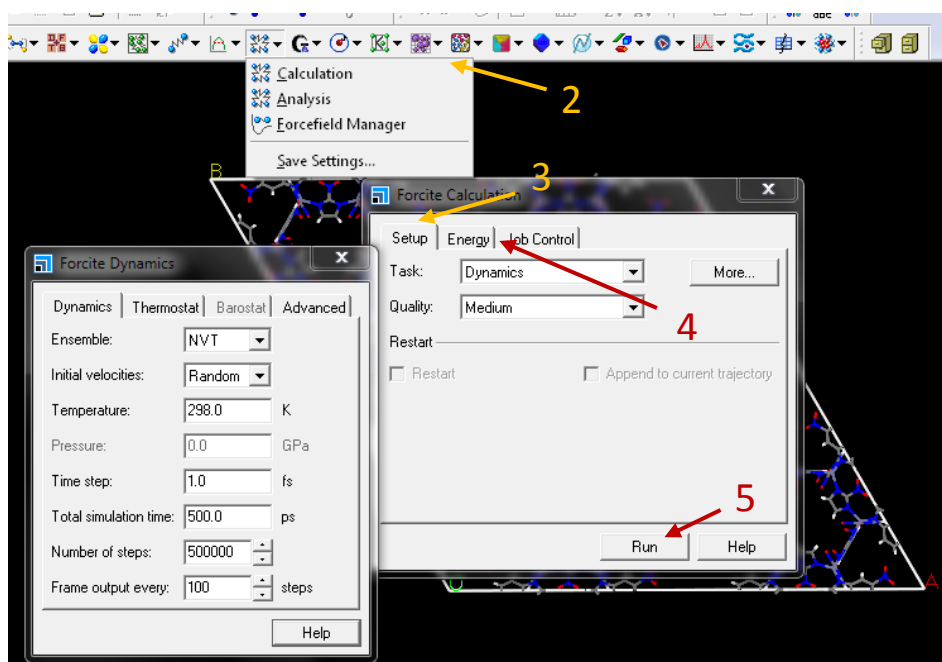


- i. Open the structure (1×1×1 unit)
- ii. Click Calculation on the *Sorption* module
- iii. In the Setup bar choose Task, Method and Quality to be Adsorption isotherm, Configurational bias and Ultra-fine.
- iv. In the Energy bar choose Forcefield, Charges and Quality to be ref 1, use current and Ultra-fine and in the Summation method choose the Electrostatic and Van der Waals to be Ewald&Group and Atom based. Choose More to change the cutoff value to be 12.5 Å.
- v. In the Job control bar click on Run to calculate the adsorption isotherm.

### 3. How to run MD simulation by Material studio.

The simulations were carried out at 298 K with the Berendsen thermostat. The cutoff radius of 12.5 Å, and a time step of 1 fs were used. The simulation times are 0.5 ns for equilibration period and 1.5 ns for the production run. The trajectories were stored every 100 steps.

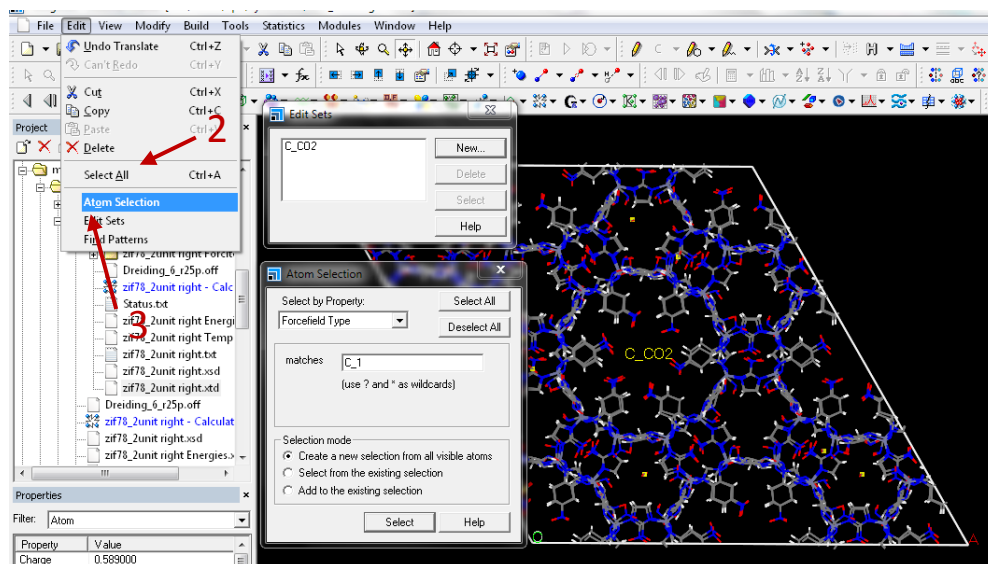
The step of calculation MD simulation was follow



- i. Open the structure (2×2×2 unit)
- ii. Click Calculation on the *Forcite* module
- iii. In the Setup bar choose Task and Quality to be Dynamics and Fine. Choose More to input the parameter as see above.
- iv. In the Energy bar choose, Forcefield, Charges and Quality to be ref 1, use current and Fine and in the Summation method choose the Electrostatic and Van der Waals to be Ewald and Ewald.
- v. In the Job control bar click on Run to calculate the MD simulation.

## 4. Evaluation

First step to achieve the results is set atom to the structure as follows



- i. open the structure (.xtd) which get from MD simulation result.
- ii. Edit set of atom by click on the edit select the “Atom selection” to choose the set of each atom *e.g.* CO<sub>2</sub>\_C.
- iii. Select on the “Edit set” to add new set of atom.

### 4.1 Radial distribution functions

A part of ZIF-78 structure which were set atom to calculate the RDF was shown in figure 3.4.

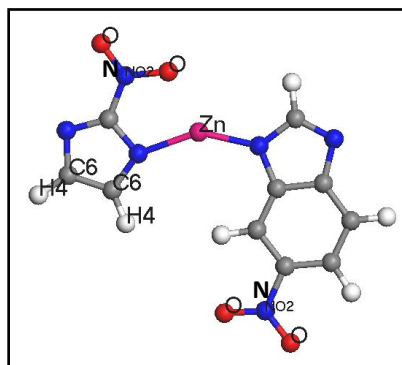
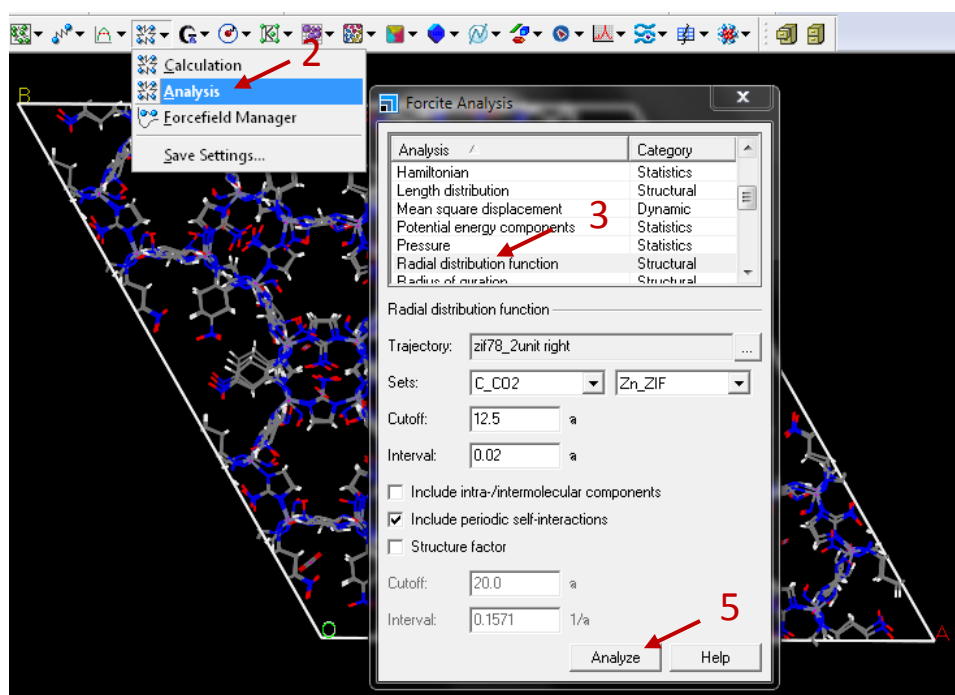


**Figure 1.** A part of ZIF-78 structure which were set atom.



To calculate the radial distribution functions which express as  $g_{ij}(r)$  is the probability to find a particle of  $j$  (the C and O atoms in CO<sub>2</sub> as well as the C and H atoms in CH<sub>4</sub>) in a sphere of radius,  $r$ , around a particle of  $i$  (the atoms in ZIF-78 lattice (Figure 1)).

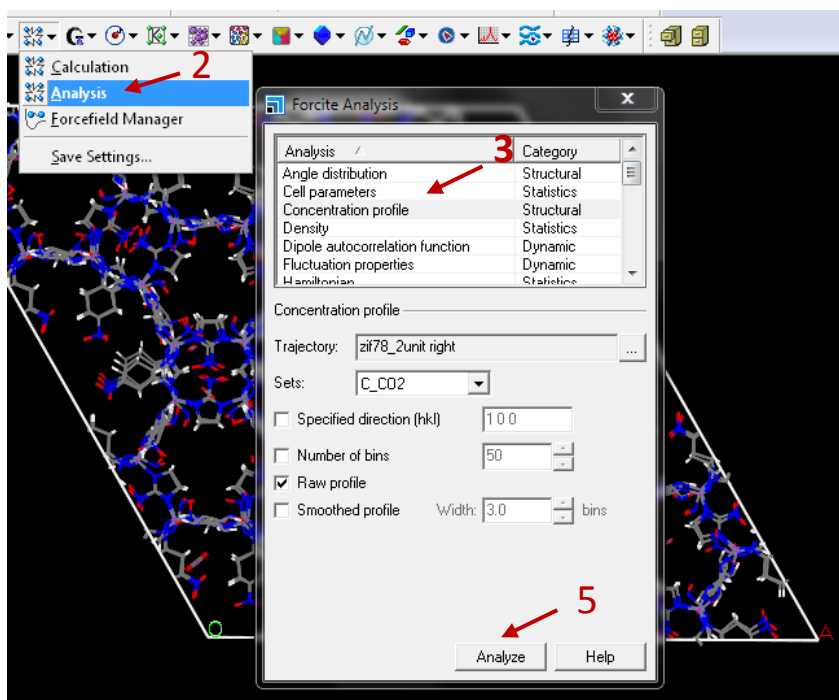
The step of calculation RDF was follow



- i. Open the structure (.xtd) which has already edit atom set.
- ii. Click Analysis on the *Forcite* module.
- iii. In the Analysis bar choose Radial distribution functions.
- iv. In the set topic choose pair of the set atom that interest and change the Cutoff to be 12.5 Å
- v. Click on Analyze to calculate RDF.

## 4.2 Probability density of molecule in z direction

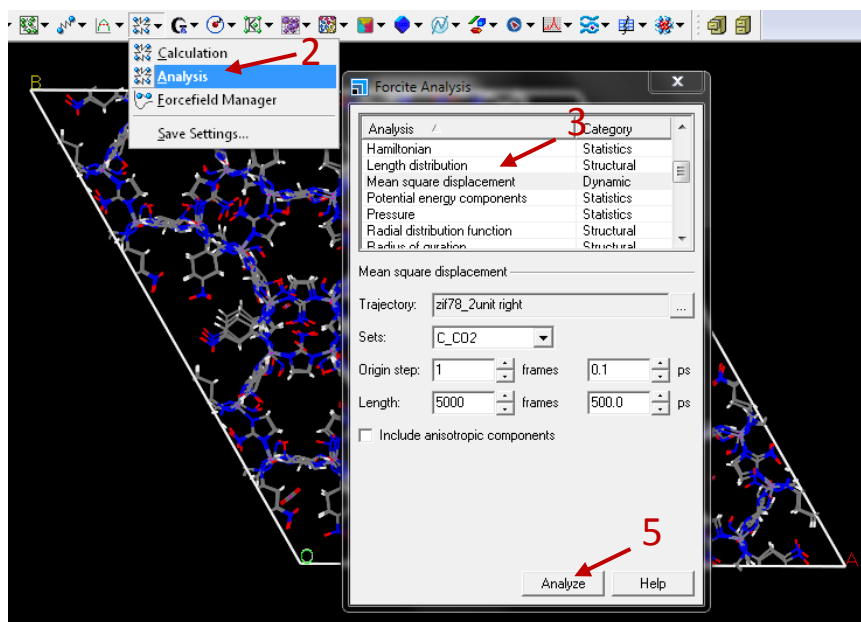
The step of analyzing probability density of guest molecule in z direction.



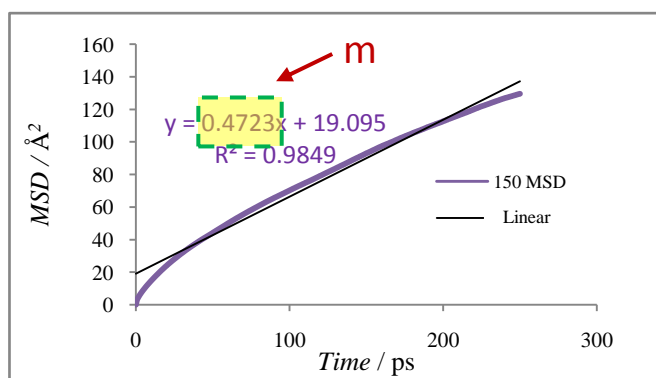
- i. Open the structure (.xtc) which has already edit atom set.
- ii. Click Analysis on the *Forcite* module.
- iii. In the Analysis bar choose Concentration profile.
- iv. In the set topic choose the set atom that interest.
- v. Click on Analyze to calculate probability to find number of guess molecule in z direction.

### 4.3 Self-diffusion coefficient

The step of analyzing self-diffusion coefficient.



- i. Open the structure (.xtc) which has already edit atom set.
- ii. Click Analysis on the *Forcite* module.
- iii. In the Analysis bar choose Mean square displacement (MSD).
- iv. In the set topic choose the set atom that interest.
- v. Click on Analyze to calculate MSD.



- vi. Plot graph between mean square displacement and time to get the slope.
- vii. Calculate the self diffusion coefficient ( $D_s$ ) by  $D_s = m/6$ .

## CURRICULUM VITAE

**Name :** Suntharee Phuangjumpee

**Date of Brith :** November 5, 1986

**E-mail address :** sun\_jan\_na@hotmail.com

### **Secondary School :**

1999-2002 Takhliprachasan School, Nakhonsawan

### **High School :**

2002-2005 Takhliprachasan School, Nakhonsawan

### **University Education :**

2005-2009 B. Eng. In Petrochemicals and Polymeric Materials, Faculty of Engineering and Industrial Technology, Silpakorn University, Nakhonpathom

2009-2011 M. Sc. In Petrochemistry and Polymer Science, Faculty of Science, Chulalongkorn University, Bangkok

### **Representative publication :**

1. Adsorption and selectivity of CO<sub>2</sub> on zeolitic imidazolate framework-78 using grand canonical monte carlo and molecular dynamic simulations. The 4<sup>th</sup> SUT Graduate Conference 2011